6 Integrated Process Design

Kai Sundmacher

6.1 Introduction

Chemical process design is a complex task because many decisions have to be taken on different levels of the process system hierarchy, that is, the molecular level, the phase level, the process unit level, and the overall process system level. Moreover, the design procedure has to be performed based on increasing levels of detail and depth of information for the procedure, which starts from the first chemical synthesis idea and ends at the final process flow sheet equipped. While computer-aided methods and tools supporting individual decision-making procedures are discussed in Chapter 5, Chapter 6 aims at presenting frameworks and workflows that enable the integration of these methods along the chemical process design pathway with a special focus on processes with liquid multiphase systems.

Section 6.2 is dedicated to general selection criteria for multiphase systems suitable for given target products or reactions to be performed. A methodology is presented that allows quantitative comparison of various types of phase systems during different stages of process design, without the need for extensive experts' knowledge. The complexity of the considered phase systems is reduced by the systematic application of questionnaires and key experiments. Thereby, process engineers are guided stepwise from the initial formulation of the problem and identification of constraints over the selection of required substrates, solvents, and additives to suitable process candidates. The whole procedure is cast into the modular computer-aided phase system selection (caPSS) framework which integrates several important aspects of process development: data acquisition, model generation, conceptual process design, flow sheet optimization, and evaluation regarding economic feasibility as well as Green Chemistry criteria.

The most important part of a liquid multiphase system, suitable for a specific homogeneously catalyzed reaction, is the identification of solvents wherein this reaction proceeds at both a high rate and high selectivity. Thus, the choice of one or multiple reaction solvent(s) is a key step in composing a powerful liquid multiphase system. Section 6.3 presents different approaches from quantum chemistry (QM) and thermodynamics to support the identification of reaction solvents. Screening of chemical equilibria or transition state barriers as a function of solvent polarizability provides insights into the reaction thermodynamics and kinetics, respectively. The methodologies presented in this section are well suited to generate a set of potential reaction solvent candidates that are combined with further solvents to obtain mixtures featuring a thermomorphic multiphase systems (TMS) behavior.

https://doi.org/10.1515/9783110709858-006

Section 6.4 discusses the integration of solvent design and process design. Usually, these two design tasks are performed sequentially, that is, first, a solvent is selected based on a limited number of desirable thermodynamic properties, and then a process is developed for this specific solvent. While computer-aided molecular design (CAMD) can aid in the selection of solvents that possess process-relevant solvent properties, only the simultaneous consideration of solvent and process design in an integrated computer-aided molecular and process design (CAMPD) framework ensures the identification of optimal process designs and operation points. In the last two decades, this realization led to the publication of several methodological developments in the scientific literature for which Section 6.4 provides an overview and illustrates key aspects in CAMD/CAMPD via selected examples.

According to the caPSS framework, one of the most important integration steps is the combination of phase system selection with model-based process synthesis. For this purpose, an integrated model-based process design methodology is presented in Section 6.5 which combines both aspects by making use of various sources of knowledge. The methodology involves an iterative workflow wherein suitable models are identified and calibrated, prior to the evaluation of the final process design, in terms of reaction and separation performance, sustainability, and economic potential. This iterative procedure repeatedly creates intermediate process design candidates based on the available information. In the case of high levels of uncertainty, model-based optimal experimental design (mbOED) is used to improve the available data basis successively via carefully designed experiments.

6.2 Selection Criteria for Liquid Multiphase Systems

Karsten H. G. Rätze, Steffen Linke, Ariane Weber, Maresa Kempin, Markus Illner, Reinhard Schomäcker, Anja Drews, Kai Sundmacher

6.2.1 Introduction

To this point, the potential of innovative liquid multiphase solvent systems for conveying chemical reactions have been demonstrated. Based on this, the development of novel chemical processes adhering to the principles of Green Chemistry is attainable. However, the adequate selection of the type of multiphase solvent system, the choice of respective compounds or additives, as well as process synthesis based on such systems remains challenging. This is mainly caused by the inherent complexity of multiphase solvent systems regarding thermodynamics, physicochemical properties, and strong interactions with reactive species. Furthermore, the selection and design of liquid multiphase systems directly affects process design in terms of required reaction equipment, separation unit sequences, and operation conditions.

Even though the reaction performance might be superior for a chosen phase system, the actual product separation and recycling of additives might hold severe obstacles, rendering a process economically infeasible or inoperable.

Considering the rather large chemical matrix of liquid multiphase systems, the necessity of an integrated process development already considering the feasibility of reaction and separation steps at an early stage and given economic and environmental constraints (Green Chemistry), process development expands to a large combinatorial problem. Given a desired target product or reaction, it is a priori unclear which multiphase solvent system is suited best. Finding optimal process variants is thus only attainable when profound knowledge on *all* considered rather complex phase systems as well as extensive comparative experimental studies is provided. This situation greatly inhibits process development and the application of such systems.

To overcome this hurdle, a holistic guideline for the systematic selection of liquid multiphase systems as reaction media and process design is presented in the following. As a major innovation, this methodology allows a quantitative comparison of multiple types of phase systems at all stages of process design, without demanding the contribution of or application by experts in the respective fields. Its application is thus designed for the industrial practitioner in the field of reaction engineering and process development, which demands fast and robust solution approaches at minimal use of resources.

To achieve this, the complexity of the considered phase systems is broken down to the systematic application of simplified questionnaires and easy to perform key experiments. The user is thus guided from the initial formulation of the problem and constraints over the selection of required substrates, solvents, and additives toward suitable process candidates in a stepwise manner at a possible minimum of required experimental effort. Simultaneously, questionnaires and key experiments already aim at identifying critical obstacles regarding the desired reaction performance, product separability, chemical stability, and operability of process candidates.

Regarding a holistic guideline, this is merged into a modular framework for the computer-aided Phase System Selection (caPSS), which systematically deploys the relevant steps for process development: data acquisition, model generation, conceptual process design, flow sheet optimization and evaluation regarding economic feasibility as well as Green Chemistry criteria. caPSS is fundamentally based on the developed methodologies and tools for the analysis, modeling, and application of phase systems. Based on these methodologies, the wrapping or deconstruction of the complex phase and reaction behavior of the investigated phase systems regarding process development is enabled and usability is increased.

The following outlines are hence restricted to the application of thermomorphic multiphase systems (TMS), microemulsion systems (MES), and Pickering emulsions (PE), which only represent a subset of possible reactive liquid multiphase systems. However, caPSS presents a major starting point for a holistic selection and design workflow for such systems and can readily be extended by adding information and

methods from respective experts for other solvent systems. As a major competing phase system, ionic liquids are mentioned by way of example for which several guidelines on their selection as solvents [19, 81] as well as for process design [63] are already available.

6.2.2 General Criteria for Phase System Selection

The general selection criteria are the first considerations after the problem statement and the chemical system definition. Independent of the selected phase system, these criteria or constraints need to be fulfilled so that they need to be evaluated in the first step. The constraints can be ordered from low effort for evaluation to higher expenditures, leading to four major steps as shown in Figure 6.1.

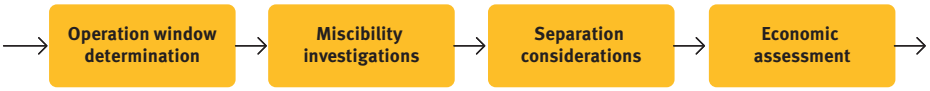

Figure 6.1: Steps for the general criteria for phase system selection.

First, the operation windows of temperature and pressure must be determined for both reaction and separation. Here, all chemicals involved in the chemical reaction are considered, that is, reactants, products, catalysts, and, if present, a ligand. Solvents are not of interest at this stage since solvent considerations are inherently phase system-specific. Melting points, boiling points, and the thermal decomposition temperature should be checked. The first lead for this information is material and safety data sheets (MSDSs). If this information is not available in the MSDSs, it should be checked if the pure components can be purchased commercially at an acceptable price to perform these rather simple experiments. If this is not possible, at least the boiling point and the melting point for reactants and products may be estimated using group contribution (GC) methods [23], while for common ligands the decomposition temperature is more relevant. Based on these data, a temperature window for operation can be roughly derived. Of course, this window may be varying for different unit operations: in a reactor, solid reactants may be unwanted, while for separation, crystallization could be an option. Regarding the pressure, the most important objective is to check the state of the reactants. The homogeneous catalyst is by definition dissolved in a liquid; therefore, all reactants need to be present in a liquid phase. Vaporous reactants may be condensed by pressure increase, or at least the gas solubility is increased for gaseous components such as synthesis gas. Deriving a pressure window from this consideration can be only done based on the expert's experience or by considering similar reactions.

Second, the miscibility of reactants should be investigated. If only one reactant is liquid within the operation window, this step can be skipped. Otherwise, it is worth studying the mutual solubilities preferably experimentally, or, if not possible, computationally using GC methods for activity coefficients (e.g., universal functional activity coefficient (UNIFAC)) or a quantum-chemical-based method such as conductor-like screening model for real solvents (COSMO-RS) [51].

Third, potential separation operations are screened for feasibility. The challenge is to separate desired products and side products from reactants and catalyst species. The simplest case is probably when the products are gaseous and can be withdrawn from the top of the reactor, as in the Ruhrchemie/Rhône-Poulenc process. This might be also achievable by distillation for some specific postreaction mixtures. If such a separation concept is worthy of consideration, the user of the methodology takes a shortcut to the systematic process design presented in Section 6.2.4. In many cases, however, this approach will not be possible, for example, due to temperature-sensitive components, and other separation techniques must be considered. Since, in the scope of this book, only liquid–liquid-based phase systems are considered, other separation techniques such as crystallization are not discussed here. In liquid–liquid-based separation, a "polarity check" must be performed for the components of interest. The goal is to estimate whether the components can be generally separated via splitting into two liquid phases. Such an estimation can be done using solubility parameters or COSMO σ-profiles. With respect to the catalyst, this polarity analysis can lead to the need to modify the ligand in order make a liquid–liquid separation feasible. A more detailed investigation cannot be conducted at this point because solvents have not yet been considered. The phase-system-specific considerations are presented in the following sections.

Finally, a rough economic analysis should be performed based on material prices. The prices P per mole for all N_{rea} reactants (rea), all N_{pro} products (pro), the catalyst (cat), and the ligand (lig) are identified in order to estimate an upper limit for the margin m per mole key reactant (key) via

$$m = X_{\mathrm{key}} \cdot \sum_{j=1}^{N_{pro}} S_j \cdot \frac{|\nu_{\mathrm{pro},j}|}{|\nu_{\mathrm{key}}|} \cdot P_{\mathrm{pro},j} - \sum_{i=1}^{N_{\mathrm{rea}}} \frac{|\nu_{\mathrm{rea},i}|}{|\nu_{\mathrm{key}}|} \cdot P_{\mathrm{rea},i} - L_{\mathrm{cat}} \cdot P_{\mathrm{cat}} - L_{\mathrm{lig}} \cdot P_{\mathrm{lig}}. \tag{6.1}$$

Here, the conversion X_{key} and the selectivity S for the desired product can be set to unity as best-case scenario or be guessed based on experience while the stoichiometric coefficients ν are taken from the reaction scheme and one reactant is chosen as a key reactant for reference. The loss of the catalyst components L_i with i ϵ {cat, lig} describes the amount of catalyst components which need to be replaced due to bleeding, deactivation, and decomposition. This replacement is done by a make-up stream in a steady-state process. Hence, the losses can be calculated from the make-up mole flux of the catalyst components and the mole flux of the key reactant using

$$L_i = \frac{\dot{n}_i}{\dot{n}_{\text{key}}}, \quad i \in \{\text{cat, lig}\}. \tag{6.2}$$

Of course, these losses cannot be determined with high certainty since they are highly dependent on the phase system and the specific process configuration applied. However, typical recovery rates for different phase systems can be found in the literature and in the case of TMS, MES, and PE, Table 4.18 provides such data. Eq. (6.1) is useful to estimate the economic potential of the selected reaction and indicates if catalyst recycling is economically necessary. Second, if the margin m is set to zero indicating a cost-covering performance, eq. (6.2) can be used to determine the order of magnitude needed for the recycling of the catalyst components. After deriving this order of magnitude, some phase systems could be discarded before advancing toward a more detailed investigation.

6.2.3 Feasibility and Constraints for Phase Systems Application and Key Experiments

The evaluation of the general criteria from the previous section limits the number of possible phase systems so that a finite set of phase system types can be investigated in more detail. Due to specific requirements for each phase system, the inclusion of a phase system in the set of feasible phase systems requires the preliminary consideration of key constraints as exemplified in Figure 6.2 and the execution of key experiments. In this section, possible preliminary considerations are discussed for three example phase systems, TMS, MES, and PE.

6.2.3.1 Thermomorphic Multiphase System

Some critical aspects must be considered for using TMS in homogeneous transition metal-catalyzed reactions. The chemical resistance of all components, especially the catalyst complex, toward the solvents and the substrates is essential. Of course, the solvents used must also be inert. The TMS technique has limitations regarding substrate concentration, amount of extractant, and limited ranges of reaction and separation temperatures (see Section 4.4). Additionally, the reaction mixture is rather diluted due to the presence of a second solvent, potentially lowering the space–time–yield. In some cases, the phase separation in the decanter is slow, leading to long residence times. In addition, the heating/cooling procedure of the reaction mixture is relatively energy-intensive.

Nevertheless, since homogeneous catalysis offers high selectivities and high catalyst activities under mild reaction conditions, it holds enormous future potential for the chemical industry. Provided an efficient recovery of the homogeneous

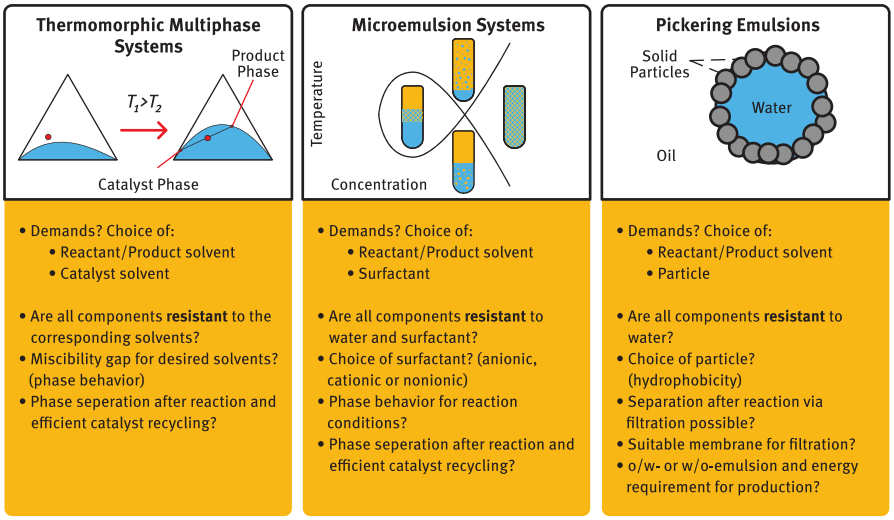

Figure 6.2: Overview of specific criteria of the considered phase systems.

catalyst, energy and waste treatment costs can be significantly reduced. The TMS technology offers an efficient way to carry out reactions under homogeneous conditions and simultaneously separate the catalyst while simultaneously being able to enable catalyst separation in a subsequent processing step.

Research on concepts such as TMSs requires significant experimental effort, implying high costs for a company in the chemical industry. The introduction of suitable key experiments can be essential to reduce the effort.

The initial point for the key experiments represents a homogeneously catalyzed reaction with an already known catalyst system. The first task is to find a suitable solvent for the reaction itself. Instead of performing experiments in the laboratory, the solvent can be found, on the one hand, by calculating the activity coefficients of the used substrates (via e.g., UNIFAC) and, on the other hand, by density functional theory (DFT) calculations of the catalyst system in different solvents. It is advisable to reduce the number of possible solvents to a minimum for this initial investigation, for instance, by a short list of suitable solvents. In the next step, the second solvent for separating catalyst and product has to be found. This solvent should not inhibit the reaction itself. Predictive calculations should be used to identify miscibility gaps between at least two compounds to reduce laboratory work. Furthermore, the solubility parameters of the used catalyst and ligand have to be calculated in the different phases along with their respective partition coefficients. These data are used to evaluate whether the solvent system found is potentially suited for separating catalyst and product in the respective system.

Finally, the TMS developed by predictive methods must be verified in the laboratory along with key parameters for its complete description. The first point should be

to map out the temperature-dependent miscibility gap before and after catalytic conversion. It needs to be proven whether the mixture is indeed homogeneous under reaction conditions with a high amount of substrate and also with a high amount of product present. In addition, a separation temperature should be determined by simple extraction experiments. If the miscibility gap fits the required reaction conditions, the next step is to carry out the reaction in the TMS. An initial reaction followed by separation should be conducted in a TMS to obtain as much information as possible with minimal laboratory effort. In this way, information on the reaction, such as yield, selectivity, and TOF, and the phase compositions after the reaction can be obtained with the aid of analytics, for example gas chromatography. In addition, the catalyst leaching into the product phase can be determined by inductively coupled plasma (ICP)-optical emission spectroscopy (OES)/MS (mass spectroscopy), so that the catalyst retention in the TMS can be confirmed. To further verify the feasibility of catalyst reuse using the TMS technique, the catalyst phase should be reused in a further reaction.

Overall, predictive work cannot replace experiments in the laboratory but it can significantly reduce the effort and, thus, the cost. The provided key experiments should form an iterative process. For example, if it is impossible to find a second solvent for the separation, the first solvent can be changed again. The concept is designed to verify the feasibility of a catalyst separation for a particular reaction via TMS. The aim is to evaluate whether further research, considering kinetic data, long-term studies, mechanistic investigations, and the selection of more environmentally friendly solvents would be appropriate. For all presented steps, specific basic knowledge is required, for example, to create a list of suitable solvents.

6.2.3.2 Microemulsion Systems

In order to carry out a homogeneously catalyzed reaction in a MES, some aspects are not predictable and need to be investigated experimentally. The chemical stability of all components, especially of the catalyst complex, to water and surfactant plays a decisive role in this application, as already described in Section 4.2.1. Probably the most important component in a MES is the surfactant. The type of surfactant, surfactant concentration, and temperature can have an enormous influence on the phase behavior and, thus, on the reaction performance as explained in Section 4.2. Furthermore, the choice of surfactant is described in Section 4.2.3.1. It must be noted that the given temperature range for the reaction already imposes a certain restriction on the choice of surfactant since not every surfactant is suitable for every temperature. Therefore, the desired three-phase area cannot always be achieved. To determine the phase behavior, it is necessary to have a look at the influence of the individual components as well as at the influence of the entire reaction mixture on the phase behavior, because the occurring effects can overlap. At the same time, the phase separation can be examined, and a suitable separation

temperature can be found in which the phases are completely and quickly separated. Inevitably, some key experiments are required to evaluate the suitability of the chosen surfactant or the concentrations and parameters. Such key experiments and suited conditions are suggested in Table 6.1.

Table 6.1: Key experiments for homogeneously catalyzed reactions in an aqueous microemulsion system.

	Changed parameter	**Reaction conditions**
Choice of surfactant	Type of surfactant and surfactant concentration Standard concentrations: 1 wt% ionic surfactant (e.g., CTAB and SDS) 8 wt% nonionic surfactant (e.g., Marlipal and Marlophen)	0.25 mol% metal precursor 1.0 mol% ligand 30 mmol substrate T, p, from literature $\alpha = \frac{m_{oil}}{m_{oil} + m_{water}} = 0.5$
Variation of substrate concentration	Adding a cosolvent, for example, octane, decane, dodecane, . . . for example: m(oil) = 25 wt% substrate + 75 wt% cosolvent	0.25 mol% metal precursor 1.0 mol% ligand 15 mmol substrate T, p, from literature

With the help of the key experiments, a rough estimation of whether the reaction can be carried out in the MES can be made. However, first, the desired yields and selectivities should be defined in the key experiments for a successful implementation. Then, if necessary, reaction conditions can be adjusted, and new key experiments can be carried out. The reaction can be optimized using various parameters such as temperature, concentrations, or a dosing strategy. However, the MES approach should not be pursued if the key experiments do not provide sufficient results.

It must be noted that the surfactants leach into the other phase, for example, into the organic phase. As a result, the catalyst complex can leach, too. Once the key experiments have been carried out successfully, the extent of catalyst leaching must be determined. This is usually done with ICP-OES but can also be done with any other common method for elemental analysis.

6.2.3.3 Pickering Emulsions

Nanoparticle-stabilized droplets and their high stability allow a robust mechanical separation of additives and catalyst via filtration in a single step and, consequently, a simpler flow sheet (Section 2.3). Also, catalysts being sensitive to mechanical stress (e.g., enzymes) can be protected [31, 92].

In order to apply PE for liquid–liquid multiphase reactions, the choice of the particle type is crucial. As introduced in Sections 2.3 and 4.3.1.1, numerous different nanoparticles are commercially available, but particle synthesis and design are also possible, which opens up several alternatives for the user, compare Table 6.2.

Table 6.2: Possible particle candidates and typical compositions for Pickering emulsion stabilization.

Alternative 1	**Alternative 2**	**Alternative 3**
Commercially available fumed silica nanoparticles of intermediate hydrophobicity (e.g., HDK series by Wacker Chemie AG)	Other commercially available particles (e.g., clay, natural emulsifiers, and spherical silica)	Particle synthesis, modification or design (e.g., Section 4.3.1.1)
Well-proven emulsion composition: 0.5 wt% particle mass fraction 0.2–0.3 dispersed phase (dp) fraction (e.g., 100 mL w/o PE, 0.5 wt% nanoparticles, 0.25 dispersed phase fraction → 0.412 g nanoparticles or 16.5 g L_{dp}^{-1})		

We recommend starting with fumed silica particles as their impact on characteristic PE properties (such as drop size distribution, stability, rheology, and mass transfer) has intensively been studied in literature and Section 4.3.1. To obtain PEs with superior long-term stability, particles have to be partially wetted by the organic and the aqueous phase (Section 2.3) and, hence, need to be of intermediate hydrophobicity. Typical emulsion compositions are given in Table 6.2. The preliminary investigation of the drop size distribution gives important information about the interfacial area available for the catalytic reaction as well as the emulsion stability. Sauter mean diameters in the low micrometer range are desirable. In a simple "drop test," in which a drop of emulsion is added to both water and the organic phase, the desired emulsion type (oil-in-water or water-in-oil) can be checked. For continuous reactions employing hydrophilic catalysts and hydrophobic substrates and products, such as the hydroformylation, with a subsequent PE filtration as investigated in Section 4.3.3, a water-in-oil emulsion is needed. In general, different dispersion devices (Section 2.3) can be applied for PE preparation. The impact of homogenization conditions using an Ultra-Turrax® on drop size distribution and rheology was investigated in Section 4.3.1.3 and 4.3.1.4.

Being the least mature of the investigated phase systems (Section 2.3), a systematic or theoretical selection of reaction conditions is not possible for PE, yet. Therefore, reaction conditions were adopted from the MES system in a first step (Table 6.1) and feasibility was demonstrated in Section 4.3.3.

PEs are known for their superior stability and are, thus, less sensitive to changes in the emulsion composition or operating conditions compared to MES and TMS. As long as the "rules" for particle choice and PE preparation (as introduced at the beginning of this section) are followed, PE stability is maintained. Sedimentation or creaming of droplets does not mean instability of the PE as simple hand-shaking or gentle stirring can redisperse the droplets. Stability against coalescence exists when the drop size distribution does not change with time.

A membrane can be chosen, for example, from the list of suitable ultrafiltration and organic solvent nanofiltration membranes (retention of micrometer-sized droplets and possibly freely suspended nanoparticle aggregates) presented in Section 4.3.1.6. Typical operating windows for these membranes are given by the manufacturers. In Section 4.3.1.6, it was shown that PE filtration is a robust process and the temperature as well as the type of the continuous phase were identified as the main influencing parameters. The PE filtration behavior was insensitive to, for example, changes in the emulsion composition (e.g., presence of reaction products) and drop sizes. This allows PEs to be optimized for the actual reaction without compromising the feasibility of PE membrane filtration.

As the catalyst should be immobilized within the dispersed aqueous phase droplets which are in turn retained 100% by the membrane, catalyst leaching is supposed to be much lower compared to MES and TMS systems (see Section 4.4). Standard methods for the quantification of catalyst and particle leaching in the permeate can be applied by the user.

6.2.4 Systematic Phase System Selection and Process Design

The general and phase system specific criteria for the TMS, MES, and PE systems represent a toolbox or heuristic to check the feasibility of these distinct phase systems for a reaction system. However, due to the limited number of considered phase systems, a generalization of these criteria is necessary as well as a systematic framework that encompasses the heuristics but allows an extension toward alternative solvent systems and their optimal application in process development.

In the initial stage of process development, information on the chemical reaction in terms of accurate thermodynamic information and reaction kinetics is limited. Nevertheless, the selection of suitable solvents or solvent systems, especially in homogeneous catalysis, is mandatory at this early stage. These solvents need to be compatible with the catalyst while simultaneously being inert to the reaction, provide favorable characteristics with respect to product separation and catalyst recovery and, ideally, possess traits that are compliant with the movement towards Green Chemistry. Due to all of these constraints, the phase system selection has significant consequences on the final process costs. Yet, this important decision is still based on expert knowledge and reference processes in contrast to systematic, model-based investigations in the

majority of cases. To systematize the selection of phase systems while retaining and embracing expert knowledge and mechanistic insight in the process, this section introduces a new and, to the best of the authors' knowledge, the first framework for computer-aided phase system selection (caPSS).

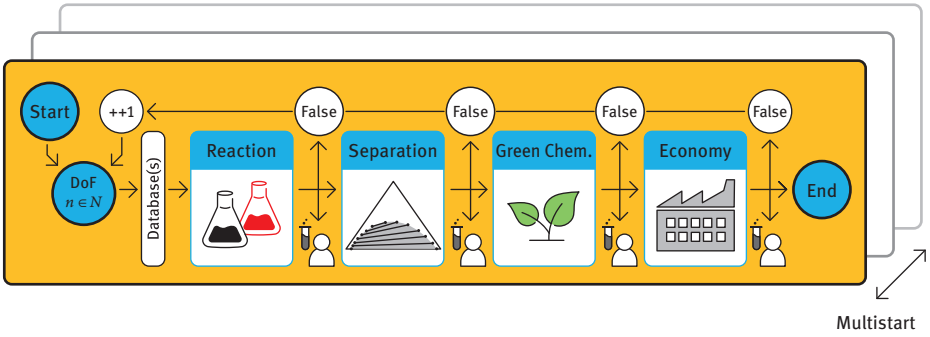

Figure 6.3: Computer-aided phase system selection (caPSS) framework. *N* denotes the set of auxiliary degrees of freedom (DoF), in particular auxiliary substances, which may be added to the reaction system. These auxiliary substances comprise catalyst ligands, solvents, surfactants, particles, and many more.

The caPSS framework aims at systematizing the process development by incorporating the steps of data acquisition, model generation, conceptual process design, flow sheet optimization, and evaluation with respect to economic feasibility and fulfillment of the goals of Green Chemistry. The practitioner is guided step by step from the initial specification of the substrates and target products to the final process or process candidates which adhere to the constraints provided. A visualization of this procedure is given in Figure 6.3. This procedure is heuristics based and favors simple processes with a minimum of auxiliary substances which are assumed to be more robust and cost-efficient. Since this heuristic may lead to suboptimal solutions in cases where increased process complexity yields significantly better economic performance, caPSS incorporates a mechanism through which the practitioner is able to override the heuristic based on prior knowledge. However, before introducing this exception, a formalization of the heuristic procedure is required. For this, we borrow the idea of the elementary process functions (EPF) methodology (Section 5.3.1.2) and express the entire process including the downstream process via an optimal control problem (OCP) in accordance with eqs. 5.32–5.36. The feasibility of this representation was already proven by Kaiser [37] in the reactor–separator network synthesis. In the OCP, $u(t) \in U \subseteq R^{n_u}$ and $\theta \in R^{n_\theta}$ denote the dynamic and static control vectors, respectively, which represent the degrees of freedom (DoF) of the process. Originally, the time coordinate was used to describe the reaction progress within the fluid element. In this generalization which encompasses the downstream process as well, the time can be considered as the

progress of the fluid element through the process or flow sheet. For the heuristic, the DoF are partitioned into inherent (inh) u_{inh}, θ_{inh} and auxiliary (aux) $u_{\text{aux}}, \theta_{\text{aux}}$ DoF. Examples for inherent DoF are heat fluxes $\dot{q}_{\text{A}}$ and diffusion fluxes j_α of all species which are part of the reaction network $\alpha \in \text{SPC}_{\text{inh}}$, while auxiliary DoF comprise diffusion fluxes j_α of species which are not native to the reaction network and, therefore, represent auxiliary substances like solvents $\alpha \in \text{SPC}_{\text{aux}}$. Of course, all inherent and auxiliary substances form the set of all species in the process $\text{SPC} = \text{SPC}_{\text{inh}} \cup \text{SPC}_{\text{aux}}$. As the name suggests, the inherent species are inherent to the reaction and process so that they can always be considered as DoF. Auxiliary DoF, on the other hand, can be added to the process to achieve a certain goal, that is, process performance, improved separability, and so on. In caPSS, this partition is used in the set N denoting the number of auxiliary DoF which can be added to the process. For example, if $N = \{1,\ 2\}$ process configurations are tested with one or two auxiliary DoF, considering the incorporation of a catalyst ligand in case of processes which face selectivity problems or, for $n = 2$, the addition of a solvent, surfactant, or particles when facing heat or mass transfer issues. With a sufficient number of auxiliary DoF, all phase systems can be composed including TMS, MES, and PE (see Table 6.3). Additionally, this concept facilitates the incorporation of prior knowledge since the practitioner defines N and ensures extensibility due to the parallel or sequential execution of multiple framework instances using multiple sets N_i as indicated in Figure 6.3.

With the introduction of auxiliary substances, substance databases are required from which suitable candidates are selected. These databases are categorized with respect to substance polarity, molecular weight, chemical activity, and so on, and provided as default databases in caPSS. However, the databases can also be extended by user-defined databases including data from literature or the key experiments (see Section 6.2.3). Depending on the allowed number of auxiliary DoF $n \in N$, the algorithm iterates through all substances from the databases in each block in Figure 6.3 to form candidate systems and test them in terms of feasibility of the reaction and separation as well as process-wide Green Chemistry and economic constraints. It is important to mention at this point that the customization of the databases allows for an initial screening with respect to Green Chemistry and economical objectives so that only promising candidates are evaluated in the framework. As already mentioned, reaction system candidates which are formed based on the substances of the initially known reaction network and the auxiliary substances are evaluated in four blocks or stages. After each block, the results comprising the set of all reaction systems passing the stage are passed to the user with additional information like distances to the constraints against which the reaction system is evaluated. In case of an empty set which is equivalent to no reaction system passing the requirements, the algorithm starts anew from the beginning with the number of auxiliary substances incremented by one according to N. This ensures that simple processes which pass all stages are preferred while allowing for the investigation of additional potential by adjusting N.

Table 6.3: Example of associations of auxiliary DoF with substance categories for a homogeneously catalyzed reaction system with selectivity problems and catalyst recovery.

Number of auxiliary DoF n	Exemplary substance categories
0	–
1	Ligand
2	Ligand + solvent
3	Ligand + two solvents (extraction, TMS)
4	Ligand + two solvents + surfactant/particles (MES/PE)

In the first stage, the feasibility of the reaction is evaluated. With the operation window (T, p) specified by the user, the reaction system is tested with respect to temperature, pressure, conversion, and selectivity constraints. The evaluation of the candidate system in each block is performed on multiple levels. For instance, if pre-implemented or user-defined models are available, simulation-based analyses are performed before experimental investigations to focus the time- and cost-intensive experiments on promising candidates. Likewise, simple models and simulations precede investigations with more sophisticated models. This allows an efficient selection process.

All auxiliary substances that pass the first stage are combined to new, reduced databases and evaluated in the second stage for checking the feasibility of the product and catalyst separation. Many homogeneously catalyzed processes require an efficient recovery of the catalyst for economic feasibility. For this task, multiple separation procedures are possible, such as liquid–liquid extraction, distillation, crystallization, and filtration via membranes to name just a few. Therefore, multiple separation technologies are investigated by simulation as well as experimentally at this stage (see Section 6.2.3 for possible key experiments for liquid–liquid separation). This can be summarized by analyzing the G/L/S-phase diagrams and evaluating constraints on the product purity and mass flow as well as catalyst recovery.

Even though Green Chemistry considerations can be included in the database creation, the entire process needs to be evaluated as well. This is necessary since substances that should not be used according to the Green Chemistry guidelines might be encapsulated in the process so that their harmful potential is drastically reduced.

Similar to the Green Chemistry considerations, the economic evaluation is performed in multiple steps. If a set of reaction system candidates is found which passes the previous stages, the operating expenses, in particular the material and energy costs, need to be estimated since they indicate trade-offs in reaction and separation performance. If the process revenue exceeds a user-defined lower limit, process development (e.g., by using the framework from Section 6.5) with the remaining

reaction system candidates commences. These rigorously modeled process candidates are then compared in terms of economic measures and Green Chemistry indicators, leading to a Pareto-front from which the user chooses a suitable final process configuration. If no candidate process suffices the user criteria, caPSS may start again with an incremented number of auxiliary DoF and/or relaxed constraints.

This procedure systematically analyzes multiphase system candidates, including various analysis techniques like model-based approaches as well as experimental investigations and focuses on the development of simple, robust, and economic processes with the inherent potential for increasing the sustainability and safety of chemicals production.

6.3 Solvent Selection for Reactions in Liquid Phases

Froze Jameel, Fabian Huxoll, Matthias Stein, Gabriele Sadowski

The choice of solvent is critical for the overall process performance with high rates and selectivity, as discussed in Section 6.2. Very often, the main emphasis when aiming at improving catalyst performance (in terms of rate, yield, and selectivity) is on modifications of the ligand. However, the many roles that solvents play in catalytic processes are receiving less attention but are equally important if not of higher relevance. The environmental impact is often considered by the incorporation of health, safety, and environment (HSE) solvent parameters into process design. The use of organic-immiscible solvents is frequently addressed with respect to catalyst recovery, product isolation, and recycling and may lead to the design and choice of a temperature-switchable solvent (a TMS).

The direct role of solvents in reactions is, however, often overlooked. The choice of solvent may affect solubilities, reaction equilibria, and transition state barriers and thus may alter kinetics and pathways and also act as a co-catalyst. The solvent molecules interact directly with the catalyst, substrates, products, and transition states, and all these interactions can increase or decrease the process rate and/or selectivity. When considering the role of solvents in catalysis, we illustrate their critical role viewed from a mechanistic approach. Physical solvent properties such as polarity and hydrogen-bond donating/accepting abilities of solvent molecules strongly influence the rate and reaction mechanism. Although frequently observed, the underlying fundamentals behind solvent effects are often not rationalized in detail. In this section, methods and tools from QM, plus the sequential incorporation of solvent effects to give the thermodynamics in ideal and non-ideal solutions, are presented.

6.3.1 Standard Gibbs Energies of Chemical Reactions and Transition State Barriers

The difference in Gibbs energies between products and reactants of a chemical reaction at standard-state conditions is the standard Gibbs energy of a reaction $\Delta_R G°$ which is directly related to the thermodynamic equilibrium constant K_a:

$$K_a = e^{-\frac{\Delta_R G^0}{RT}} \tag{6.3}$$

Thus, a negative standard Gibbs energy of a reaction refers to a chemical equilibrium on the product side, whereas a positive $\Delta_R G°$ indicates that the unreacted substrates are preferred. Standard Gibbs energies of reactions, and thus chemical equilibrium constants, for a particular reaction, are often not available experimentally. Qualitative and quantitative approaches to obtain $\Delta_R G°$ for a new type of reaction from a theoretical perspective are then an attractive alternative to time-consuming and difficult experiments.

The standard Gibbs energy of a reaction $\Delta_R G°$ is introduced here to describe the reaction of two compounds "A" and "B" forming the product "C" (Figure 6.4) as the difference in standard Gibbs energies between product "C" and reactants "A" and "B". Before reaching the product state "C", reactants "A" and "B" form a transition state $[A–B]^‡$ which further reacts toward the product "C". The transition state theory treats the transition state as a quasi-equilibrium state (eq. (6.4)). Thermodynamics and kinetics of a chemical reaction cannot be treated separately since they are closely related by changes in standard Gibbs energies, the latter by that of the formation of the transition state $[A–B]^‡$, for example, the transition state barrier $\Delta_R G^‡$:

$$k = \left(\frac{k_B\ T}{h}\right) \kappa(T)\ e^{-\frac{\Delta_R G^‡}{RT}} \tag{6.4}$$

Here, k is the reaction rate constant, $\kappa(T)$ represents the collision factor, k_B is Boltzmann's, and h is Planck's constant.

6.3.2 Introducing a Three-Level Description of Chemical Reactions in Solution

In the following, we are introducing a three-level description for systematic incorporation of solvent effects on the thermodynamics, here the standard Gibbs energy of a reaction $\Delta_R G°$, and the kinetics, here the Gibbs energy of the transition state barrier $\Delta_R G^‡$ (Figure 6.4). The top level is the chemical reaction when treated in the absence of any solvent. $\Delta_R G^{o,id}$ can be obtained from various theoretical approaches. Reactants $A_{(g)}$ and $B_{(g)}$ form a transition state $[A–B]^‡_{(g)}$ and the product $C_{(g)}$, where (g) denotes

the neglect of any chemical environment, commonly referred to as the "ideal-gas phase". Even for the gas phase, a careful benchmarking of computationally efficient DFT methods versus wave function-based solutions of the electronic Schrödinger equation may reveal systematic or non-systematic deficiencies of the former (Section 3.2). Standard Gibbs energies of reacting species (reactants, transition states, and products) are obtained by adding thermodynamic corrections to electronic energies via partition functions from statistical thermodynamics, for example, based on the rigid rotor and harmonic oscillator assumptions. QM calculations in the gas phase (g) are able to provide transition state barriers (e.g., the thermodynamics of activation) and the thermodynamics (standard Gibbs energies; chemical equilibria) of the overall reaction in an ideal gas phase with an uncertainty of 5–10 kJ mol^{-1}.

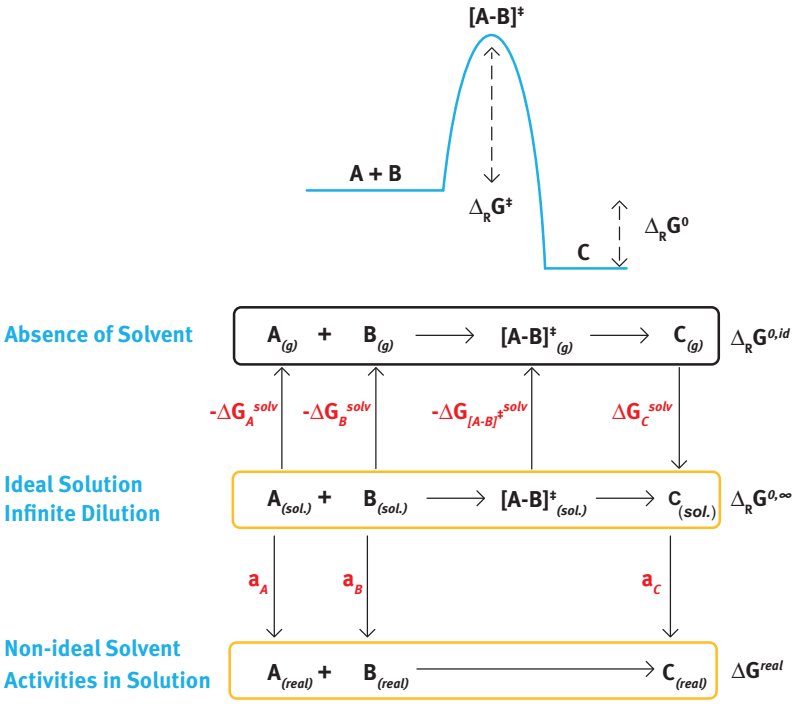

Figure 6.4: Three-level workflow of the treatment of chemical reactions in condensed phases. QM calculations of standard Gibbs energies of activation and standard Gibbs energies of reactions $\Delta_R G^{o,id}$, in the gas phase (g) are corrected by solvation terms ΔG_i^{solv} in order to describe the reaction at infinite dilution ($\Delta_R G^{o,\infty}$). Thermodynamic activities a_i of the reactant and product species are used to obtain the standard Gibbs energy of a reaction in a real (liquid) solvent (ΔG^{real}).

6.3.2.1 Taking Quantum Chemical Calculations from the Gas Phase to Infinitely Diluted Solution

The second level is the incorporation of solvation effects into the QM approach to obtain the Gibbs energies of the individual species $A_{(sol)}$, $B_{(sol)}$, and $C_{(sol)}$ in solution, but also the one of the transition state $[A–B]^{‡}_{(sol)}$ (Figure 6.4). Solvation effects can be incorporated using various approaches (Figure 6.5). The accuracy of QM methods to calculate standard Gibbs energies of reactions in condensed-phase environments is still a challenge and ongoing research. The simplest and computationally most efficient one is the description of solvent effects by a dielectric continuum such as in COSMO (conductor-like solvation model) [52]. Polarization of the solute by surrounding solvent molecules is described by an unspecific term depending on the dielectric constant ε. Continuum solvent models represent an appealing approach for the calculation of Gibbs energies of solvation, in particular for relative effects upon change of solvent or temperature.

Such a consideration of solvation gives the infinitely diluted solution of non-interacting species in which molecular solute–solute and solvent–solvent interactions are not incorporated. This state refers to an "ideal solution at infinite dilution" to give $\Delta_R G^{o,\infty}$ or the respective transition state barrier $\Delta_R G^{‡,\infty}$. Going from accurate QM calculations in the absence of a solvent to chemical reactions in solution is performed via a Born–Haber cyclic approach. For the thermodynamics and kinetics of the reaction to be calculated in solvents, reactants A and B are (de)solvated from an infinitely diluted solution to the gas phase (by $-\Delta G_{A,B}{}^{solv}$), and subsequently, the transition state $[A\text{-}B]^{‡}$ ($\Delta G^{solv}{}_{[A\text{-}B]‡}$) and the product C (by $\Delta G_C{}^{solv}$) are solvated to yield the standard Gibbs energy at infinite dilution but also the effect of (de)stabilization of the transition state (Figure 6.4).

Figure 6.5 shows different levels of representations of solute–solvent interactions in QM calculations. The dielectric continuum representation (left) is a computationally affordable approach to incorporate polarization effects into the electronic Schrödinger equation. The most realistic one is the full explicit atomistic QM treatment of all solute, solvent, and catalyst species in a large simulation box with periodic boundary conditions. The mixed cluster-continuum model (hybrid; right) is an intermediate level representation in which solvent molecules close to the solute are treated in full atomistic detail whereas further distant solvents are a dielectric medium.

6.3.2.2 From Infinite Dilution to Real Solutions with Thermodynamic Activities of Reacting Species

The third level of solvent treatment is a correction for the "non-ideality" of the previous stages. The "real solvent" description, which explicitly considers intermolecular interactions among all species in solution, is obtained from experimentally parameterized

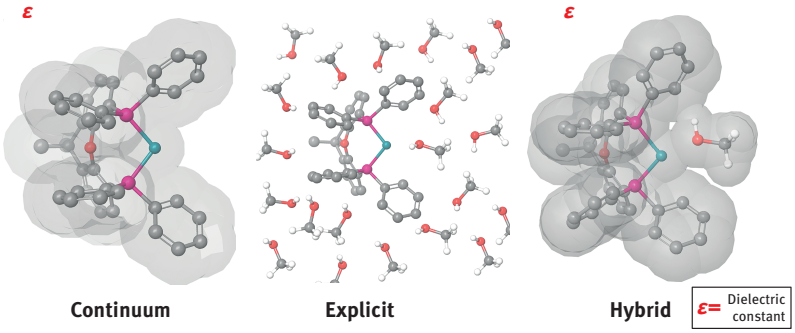

Figure 6.5: Different levels of solvent representations in QM calculations. Left: continuum solvent model with a specific dielectric constant ε; center: the explicit atomistic picture of all solute and solvent molecules; right: mixed cluster-continuum model in which the solute (here a catalyst) and directly interacting solvent molecules are embedded in a dielectric medium.

coarse-grained analytical models, for example, perturbed-chain statistical associating fluid theory (PC-SAFT, Section 3.1.1) or the group-contribution method modified UNIFAC-Do. This computationally efficient treatment of chemical species in solution yields the thermodynamic activities a_i of the reactants and products in different solvents (Figure 6.4). However, this does not include the transition state.

The solvent influence on reaction equilibria in real solutions was already discussed in Section 3.1.5. The reaction rate r of an equilibrium reaction $A + B \rightleftharpoons C + D$ is defined in a thermodynamic-consistent way using thermodynamic activities instead of concentrations (eqs. (3.70)–(3.72)). At the beginning of the reaction ($t = 0$), k_{-1} can be neglected if no products are present in the mixture. Thus, eq. (3.70) can be simplified to

$$r = k_1^* \cdot a_A \cdot a_B \tag{6.5}$$

As solvent effects on the reactants are accounted for by the thermodynamic activities a_i, the intrinsic reaction rate constant k_1^* does not depend on the solvent as long as the transition state is not affected by the solvent. In these cases, it is possible to predict the solvent influence on the reaction kinetics from the reactant thermodynamic activities only. The highest reaction rates and turnover frequencies are obtained in solvents that cause high reactant thermodynamic activities, that is, large activity coefficients of the reactants. Thus, potential solvents were screened toward their effect on the thermodynamic activity of the reactants in a reaction mixture.

Examples of high practical relevance are the hydroformylation of olefins and the subsequent reductive amination of aldehydes. These are homogeneously catalyzed liquid-phase reactions with the gases CO and/or H_2 as reactant(s). Thus, the thermodynamic activity of these gaseous components in the liquid also needs to be accounted for. However, it could be shown that – except for very high pressure – the

thermodynamic activity of gaseous components in the liquid phase does only depend on the composition of the gas phase which is in equilibrium with that liquid [34]. Consequently, in contrast to their solubility, the thermodynamic activities of the gases CO and H_2 neither depend on the solvent nor on the composition of the liquid phase. Thus, as long as liquid-phase reactions are performed in the presence of an equilibrium gas phase, the solvent influence on the reaction is only determined by the solvent influence on the thermodynamic activities of the reactants in the liquid solution.

6.3.3 Solvent Selection for Chemical Equilibria and Reaction Rates

The rationale to suggest an optimal solvent for a given chemical reaction is based on the many roles a solvent may play. Differences in Gibbs energies of solvation between substrates and products affect the standard Gibbs energy of the reaction $\Delta_R G°$ and thus the chemical equilibrium. The transition state barrier of the rate-determining step $\Delta_R G^{\ddagger}$ should be minimal to yield fast kinetics of the chemical reaction. Likewise, high thermodynamic activities for reactants (a_i) are in favor of a swift catalytic turnover. There may also be direct molecular interactions between solvent molecules and a catalyst to (i) act as a cocatalyst, (ii) stabilize the transition state structure, or (iii) inhibit catalytic performance. Here, we present selected examples of the different roles that solvents may play in catalysis.

6.3.3.1 Modeling Solvent Effects on Standard Gibbs Energies and Chemical Equilibria

The solvent effects on the hydroformylation reaction of 1-dodecene to *n*-tridecanal were investigated at different decane/DMF ratios and different temperatures [55]. Solvent effects were described using those two apparently different approaches: first, a qualitative prediction and, second, a quantitative prediction, whereas the qualitative prediction is based on the standard Gibbs energy of reaction at infinite dilution in liquid solvents. The standard Gibbs energy of reaction at infinite dilution in liquid solvents was also calculated using the fugacity coefficients at infinite dilution calculated from PC-SAFT.

Quantum chemically calculated standard Gibbs energies of reaction in absence of any solvent $\Delta_R G^{0,id}$ were calculated using various levels of theory, and a high level of electron correlation was required to obtain results of chemical accuracy (within 4 kJ mol^{-1}). Thermochemical properties for the hydroformylation reaction of 1-dodecene were calculated at various levels of accuracy to critically assess their performance. DFT calculations and wave function-based methods with different levels of electron correlation were used for those tasks. Calculation of second derivatives was performed to consider thermodynamic corrections to the energies at 298 and 378 K.

Solvent effects were treated using an implicit solvation model to estimate the effect of solvents on the standard Gibbs energy of reaction at infinite dilution in liquid solvents. The consideration of solvents at infinite dilution in liquid decane/DMF solvent mixtures ($\Delta_R G^{0,\infty}$) allowed a qualitative prediction of the solvent effect on the equilibrium concentrations (Table 6.4). Based on the standard Gibbs energy of reaction at the ideal-gas standard state and on fugacity coefficients φ_i calculated using PC-SAFT, the equilibrium concentrations of reactants and products for the 1-dodecene hydroformylation performed in decane/DMF mixtures at different compositions could be predicted in very good agreement with experimental data (Section 3.1.5).

Table 6.4: Standard Gibbs energies for the hydroformylation of 1-dodecene at infinite dilution in liquid solvent mixtures decane/DMF at 378.15 K.

w/*w* (decane/DMF)	*p* (bar)	$\Delta_R G^{0,\infty}$ (kJ mol^{-1})	
		MP2/COSMO	PC-SAFT
80/20	0.74	−36.48	−68.76
0/100	0.57	−37.72	−79.18

The values obtained from the two methods agree qualitatively, but differ in absolute values and also regarding the magnitude of the solvent effect. While PC-SAFT explicitly accounts for binary interactions among the solvents and the reacting species, COSMO is an implicit solvation model in which the reacting species are embedded in a dielectric continuum surrounding the molecular cavity. COSMO, in contrast to PC-SAFT, does not explicitly include solvent molecules. Nevertheless, the standard Gibbs energies of reaction at infinite dilution decrease with increasing DMF content for both MP2/COSMO and MP2/PC-SAFT, which leads to increasing K_a. This is in qualitative agreement with the experimental observations. This shows that the solvent effect on the reaction equilibria can be predicted qualitatively via QM calculations alone as well as via a combination of QM calculations and PC-SAFT without using any experimental reaction data.

Table 6.5: Thermodynamic equilibrium constants for the hydroformylation of 1-dodecene at ideal-gas standard state.

T (K)	$K_{f;MP2}$	$K_{f;exp}$
368	848.85	973.08
378	292.97	322.82
388	106.65	129.34

A quantitative prediction of the solvent effect on K_x requires the thermodynamic equilibrium constant K_f. K_f was calculated at different temperatures using the reaction enthalpy and the Gibbs energy of reaction at the ideal-gas standard state. The standard Gibbs energy of reaction was used to determine the thermodynamic equilibrium constant K_f at 378 K. K_f values at 368 K and at 388 K were determined using the standard reaction enthalpy at 373 K and 383 K, respectively. For comparison, thermodynamic equilibrium constants $K_{f;exp}$ were calculated using the experimentally determined mole fractions of the reactants/products at the solvent composition 60%/40% (w_{decane}/w_{DMF}) and the respective fugacity coefficients obtained from PC-SAFT (Section 3.1.5). The resulting two sets of values for the thermodynamic equilibrium constant from both, MP2 ($K_{f;MP2}$) and experimental data combined with PC-SAFT ($K_{f;exp}$) are presented in Table 6.5. As can be seen, the values obtained from MP2 calculations and experimental data/PC-SAFT are in very good agreement, particularly keeping in mind the complexity of the reaction system and that QM is purely predictive. The solvent effect observed could not have been described at all neglecting the fugacity coefficients, as these are the only physical properties that depend on the solvent and therewith enforce the change in K_x.

6.3.3.2 Model-Based Screening to Predict Solvent Effects on Reaction Kinetics

Here, we present two examples of the application of the combined solvent screening using QM and UNIFAC-Do. Both refer to complex reaction systems in homogenous catalysis using substrates from renewable sources.

According to the above-defined criteria, the optimum solvent must simultaneously provide high thermodynamic activities of the liquid reactants (eq. (6.5)) and low activation barriers according to eq. (6.4).

Hydroformylation

For the Rh(I)-BIPHEPHOS catalyzed hydroformylation, 12 commonly used polar and non-polar industrial solvents were screened in terms of their effect on the thermodynamics and kinetics of the reaction (Figure 6.6a). The thermodynamics of the reaction is significantly affected by the choice of solvent. A COSMO screening of the effect of polarity on the Gibbs energy of the reaction $-\Delta_R G^{0,\infty}$ was ~ 12 kJ mol^{-1} [36]. Polar media, such as DMF, NMP, and methanol, appear to be beneficial for the thermodynamics of the hydroformylation reaction.

The solvent polarity can also affect the activation energy of the rate-determining step (Figure 6.6a) when the stabilization of the transition state is more pronounced than that of the preceding intermediate. In Figure 6.6a, the reduction of the transition state barrier $-\Delta\Delta G_{[A-B]\ddagger,(sol)}$ upon screening of the dielectric constant ε relative to that in the absence of solvent is given. The activation energy of the rate-determining step

in the hydroformylation reaction, that is, the hydride insertion into the olefin double bond, is not significantly affected by the polarity of solvent (only by ~4 kJ mol^{-1}) which is in good agreement with the experiment.

UNIFAC-Do calculations were performed to obtain the thermodynamic activity of 1-decene in reactions mixtures for the same solvents at experimental reaction conditions (100 °C, 13 wt% 1-decene). The results are depicted in Figure 6.6a, emphasizing a significant solvent effect on the thermodynamic activity of 1-decene in various solvents.

Based on these calculations, DMF, NMP, and short-chain alcohols, especially methanol, are predicted to be promising solvent candidates for hydroformylation. Performing the reaction in one of these solvents should lead to a fast conversion from the reactants to the desired product. In contrast, solvents like THF, toluene, or *n*-heptane are expected to result in lower reactant-conversion rates.

Reductive Amination

As a second example, we present results for the reductive amination of undecanal with diethylamine (DEA) in the presence of Rh(I)-XANTPHOS. While the chemical equilibrium is hardly affected by the polarity of solvent (only by ~2 kJ mol^{-1}) [7, 34], the rate of reduction of the enamine is critically dependent on the solvent polarity. Polar media accelerate the rate of the reaction by lowering the transition state barrier and thus increase the overall yield of the reaction. The rate constant of the rate-limiting reduction step increases by an order of magnitude depending on the polarity of solvent (Figure 6.6b), which is in good agreement with the experiment [34].

UNIFAC-Do screening of the solvent effect on the reaction kinetics of the reductive amination of undecanal was performed. The reductive elimination of the tertiary amine was found to be the rate-determining reaction step [49]. Thus, the thermodynamic activity of the enamine intermediate in various solvent candidates was evaluated. UNIFAC-Do calculations were performed for the thermodynamic activity of the enamine in the reaction mixture, considering 12 different solvents and fixed initial reactant concentration (4 wt% undecanal, and fourfold excess DEA). Short-chain alcohols, NMP, and DMF are predicted to lead to high reactant-conversion rates, similar to the results of the hydroformylation. THF, toluene, and *n*-heptane, again, perform inadequately for this reaction and should, if possible, not be considered as solvents for these reactions.

When combining results from QM and UNIFAC-Do solvent screening of the hydroformylation and reductive amination reactions, the two, apparently contradictory approaches give a consistent picture. The combined results are shown in Figure 6.6a for the hydroformylation and in Figure 6.6b for the reductive amination. As a result of initial screening, polar solvents are preferred candidates compared to non-polar solvents for both example reactions. DMF, NMP, and methanol show similar performance in

terms of reduction of activation energy for the rate-determining step making the recommendation of a single most appropriate solvent not possible at this state. However, as a result of swift solvent screening, the number of solvents to be considered in a subsequent step is significantly reduced.

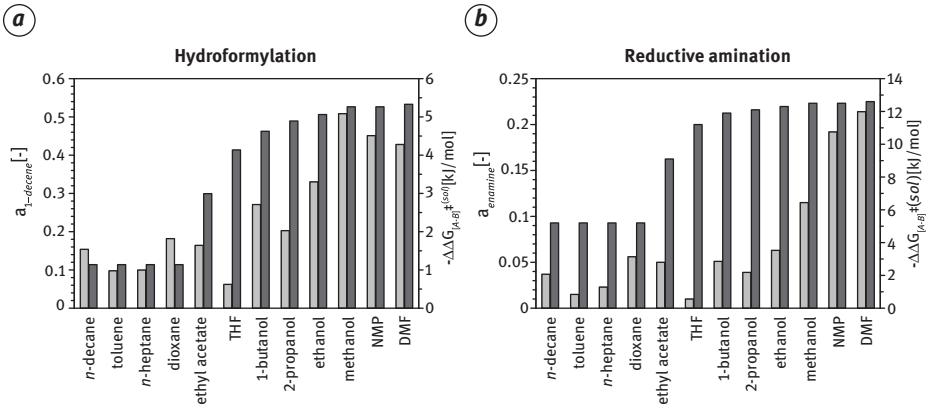

Figure 6.6: Solvent effects on (a) the rate-determining step of the hydroformylation (b) and the reductive amination. Thermodynamic reactant activities were calculated using UNIFAC-Do (left axis, light gray bars) and reduction of the transition state barrier relative to those in absence of solvent (right axis, dark gray bars) in 12 different solvents [34].

6.3.3.3 Beyond Implicit Solvation: The Many Roles of Solvent Molecules

Accelerating and Promoting Catalysis

The Pd(II)-catalyst hydroesterification of 1-decene with methanol and 1,2-bis(di-tert-butylphosphinomethyl)benzene is a prime example for the promotion of catalysis by solvent molecules (Figure 6.7). In the pre-catalyst, a methanol solvent molecule is coordinating to the central metal atom and blocking the site of catalytic turnover. Here, methanol plays three different roles in this catalytic process: first, its dissociation is necessary to activate the pre-catalyst; second, it is the substrate to form methoxy esters; third, it coordinates to the Pd(II)-hydride intermediate complex and occupies the vacant coordination site. In the rate-limiting final step of methanolysis, the coordination of two additional methanol molecules was investigated in a mixed cluster/continuum model. The cyclic arrangement of these two additional solvent molecules is the optimal coordination geometry to form a network of three hydrogen bonds in addition to the substrate–Pd interaction. The thermodynamically unfavorable single methanol coordination (Gibbs energy of reaction step +31 kJ mol^{-1}) becomes thermodynamically feasible (by –3.4 kJ mol^{-1}). The explicit solvent methanol molecules form a cyclic ring cluster which enables an efficient concerted proton transfer from methanol to the palladium center to regenerate the hydride [35].

One prime example for explicit solvent stabilization of the transition state is the amination step of undecanal with DEA using methanol as a solvent (Figure 6.7). The Gibbs energy of the transition state barrier of the hemiaminal formation by the nucleophilic addition of DEA to undecanal is critically dependent on an assisted proton transfer by explicit solvent coordination. The transition state barrier is +137 kJ mol^{-1} in the absence of any explicit solvent coordination and reduces to +41 and +19 kJ mol^{-1} when one or two methanol molecules, respectively, are assisting the proton transfer from the amine to form the hemiaminal intermediate [34].

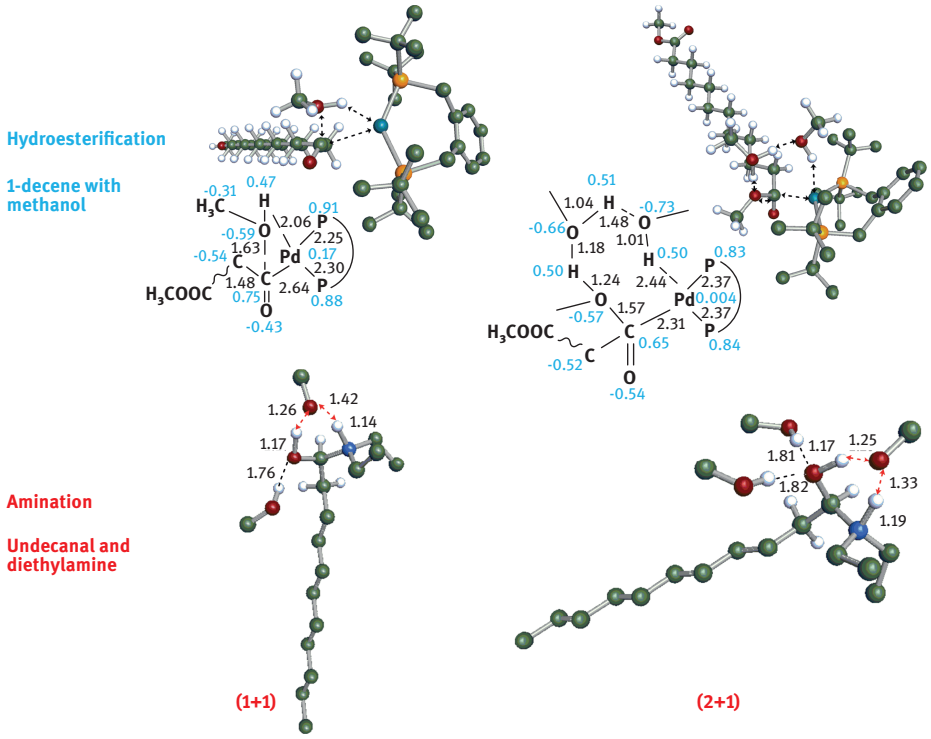

Figure 6.7: Two examples of explicit solvent involvement in catalysis (top). Explicit methanol solvent molecules acting as proton transfer agents in methanolysis of the acyl species (rate-determining step) in the hydroesterification of methyl 10-undecenoate (bottom) . Hydrogen bond-forming methanol solvent molecules in the amination reaction of undecanal with diethylamine. One methanol molecule is acting as a proton transfer mediator, two methanol molecules from hydrogen bonds with the carbonyl oxygen and thus assist the nucleophilic addition of the amine.

Catalyst Inhibition

Solvents in chemical reactions have a multitude of roles: solubilizing substrates, catalysts, and products; stabilizing intermediates and transition states; enabling a facile separation of catalyst and products, and so on. An aspect that has not received much

attention yet is the inhibition of catalysts by solvent molecules, and the thermal decomposition of solvents.

Methanol, NMP, and DMF were top-ranked candidate solvents for the reductive amination (Section 6.3.3.2). Methanol and DMF were chosen for further investigations as representatives of polar media with and without hydrogen bonding abilities. The active transition metal catalyst has a vacant binding site where the substrate must coordinate for the reaction to proceed. This site is, in principle, also solvent accessible and solvent molecules may approach the central metal atom and thus occupy the site of catalytic turnover. If such binding is overstabilized, solvent coordination competes with substrate binding. Since the concentration of active transition metal catalysts in solution may be lower than estimated, overall turnover and reaction yields will be affected.

Table 6.6 shows the DFT calculated binding energies of various species to the active catalyst for the reductive amination reaction. Enamine is the substrate and also has high binding energy to the Rh(I) catalyst. Carbon monoxide is an inhibitor and shows the highest binding energy. For the reduction of the enamine, H_2 must coordinate to Rh(I) and undergo an oxidative addition. DMF, as a frequently used solvent, has higher binding energy to the active catalyst than hydrogen and is thus a competitor. Methanol, as an alternative solvent candidate, has lower binding energy and does not obstruct hydrogen coordination. It is not competitive with either substrate or H_2 binding and is not expected to inhibit the catalytic performance. As discussed above, the hydrogen bonding ability of methanol also significantly reduces the activation barrier for enamine formation.

At elevated temperature and pressure, DMF is not an inert solvent but is also susceptible to decomposition into dimethylamine and carbon monoxide. These DMF decomposition products can also potentially bind to the catalytic center, further reducing the catalytic activity of Rh(I) (Table 6.6). Hence, the use of DMF as a solvent is not recommended for the hydrogenation of the enamine.

Table 6.6: Calculated binding energies of various species during reductive amination to the Rh(I)XANTPHOS catalyst in kJ mol^{-1}.

Enamine	H_2	MeOH	DMF	DMA	CO
−125	−61	−50	−81	−97	−183

The reaction performance was confirmed by experiments comparing methanol, DMF, toluene, *n*-heptane, and 1-butanol as solvents. The reductive amination of undecanal with DEA in different solvent systems showed that methanol gave the highest product yields and lowest side-product formation [34].

6.3.4 Conclusions

The multifaceted roles of solvents in integrated process design need adequate computational treatment. As outlined above, the development of a generally applicable thermodynamic multistep workflow allows a fast solvent screening without the need for *a priori* experimental reaction data. The presented approach can be a powerful tool in selecting optimal solvents for catalytic transformations and significantly reduce time-consuming experimental solvent screening.

Different methods and levels of treating solvent effects in catalytic reactions give different levels of information. Screening of chemical equilibria or transition state barriers as a function of solvent polarizability gives initial valuable insight into reaction thermodynamics and kinetics, respectively. Calculating the thermodynamic activity of reactants in (mixed) solvents is a complementary approach. Solute–solute, solvent–solute, and solvent–solvent interaction parameters are included in this "real solvent" representation whereas the catalyst is not considered.

Ideally, both approaches give a consistent set of solvent candidates of which only the top-ranked might be evaluated experimentally. Only when explicit coordination of solvent molecules, their active involvement in transition state stabilization, or reaction mechanism appear possible, a final full atomistic representation of solvent molecules in QM is required. However, for integrated process design, the methodologies presented in this section are very well-suited to create a list of reasonable solvent candidate molecules.

6.4 Integrated Solvent and Process Design

Steffen Linke, Tobias Keßler, Christian Kunde, Achim Kienle, Kai Sundmacher

As one part of the procedure for selecting an appropriate phase system for homogeneously catalyzed reactions, as proposed in caPPS in Section 6.2, the specific problem of selecting a solvent or a solvent mixture for a particular phase system must be investigated. Traditionally, in chemical process development, solvents are selected based on preliminary studies, considering some desirable thermodynamic properties for decision-making. Subsequently, a process is developed for the selected solvent. This sequential procedure can lead to suboptimal decisions since complicated trade-offs must be made between different thermodynamic properties that can only be rationally weighted at the process level for each solvent individually. Therefore, it is recommendable to develop and establish methodologies that combine very closely solvent selection with the process design procedure. This integrated approach and the related frameworks published in the scientific literature are discussed in the following section and are illustrated by specific examples from the authors' research works.

6.4.1 Introduction to Integrated Solvent and Process Design

Integrated solvent and process design, or CAMPD, means selecting a solvent by evaluating its performance at the process level so that all interdependencies, for example, between different unit operations, are considered. This performance can usually be defined as economic profit as a rule, but exergetic considerations, ecological criteria, or even multiobjective trade-offs are also possible. Besides the decision criterion, engineers must choose the solvent design space, a method to predict thermodynamics, unit operation models, the process flow sheet, an optimization algorithm, and the degree of decomposition. The solvent design space defines what kind and type of molecules are considered and studied as solvent candidates; in other words, the design space is the pool of molecular possibilities for the solvent. Property estimation models are necessary to predict the thermodynamic behavior of the molecules in mixtures. Therefore, the process performance of a solvent can be calculated without experimental data, and a selection can be made in the early stage of process design. Besides physical properties, HSE criteria are also very important in decision-making, and thus, predictive methods are needed for these properties as well. Regarding the process, models for the unit operations must be chosen describing, for example, reactors, separators, and heat exchangers. Obviously, these unit operations need to be connected resulting in a process flow sheet. If an economic analysis is performed, cost models for the apparatus and the utilities must be formulated as well. Since individual process simulations for each solvent candidate are not sufficient for fair decision-making, an optimization algorithm must be applied. Such an algorithm must be able to handle and solve the system of equations representing the process flow sheet for each solvent candidate under investigation.

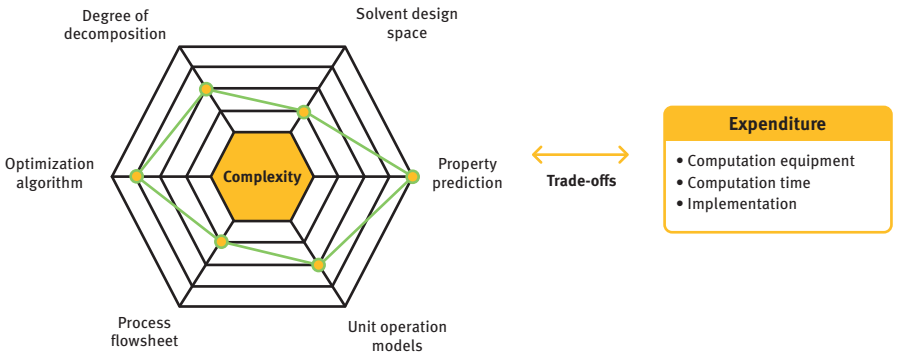

Figure 6.8: Trade-offs in the context of integrated solvent and process design between the scope of the results, their accuracy, and the effort required to solve the optimization problem.

In total, engineers face a bundle of different trade-offs between accuracy, reliability, the scope of the results, and the expenditure required including man and computational power, which are summarized in Figure 6.8. To give an example, a huge process network consisting of fully spatially resolved unit operations, applying complex quantum mechanical (QM) calculations for the solvent, and solved to global optimality is conceivable but not practically viable nowadays. Therefore, reasonable trade-offs must be made by the expertise of the engineers involved, such as the use of shortcut models for unit operations. A common technique to make the problem feasible is to apply decompositions, that is, to reduce the level of integration, and, thus, the complexity. This leads to smaller or simpler problems, which are solved to identify promising solvent candidates and starting values for the more complex, fully integrated solvent-process problem.

If these challenges are met, unexpected and highly efficient solvent and process configurations may be found that lead to benefits on a major scale. However, from a practical point of view, it must be considered that a solvent is always an auxiliary component, which must be cheap and easily available in large quantities. Secondly, new components being considered for large-scale use must be carefully studied from a regulatory perspective resulting in costly experiments and authorization processes. Thirdly, all side effects that occur in chemistry are up to now not predictable, so that complex solvents and mixtures may be predicted to be beneficial but will not work in practice. The experimental validation of the prediction is consequently essential, as well as the initial restriction to predictable chemistry. Therefore, the direct impact of integrated process and solvent design in practice may finally be more in the direction of identifying generally useable solvent structures for many applications, rather than designing one specific solvent for each process, or, on the other hand, to replace widely used solvents which have drawbacks due to their HSE properties and are becoming more strictly regulated.

Mathematically spoken, an integrated solvent-process design problem can be formulated as optimization problem as shown in eqs. (6.6)–(6.14) adapted from Austin et al. [3]:

$$\min C(n,p,\mu) \tag{6.6}$$

$$p = f(n,\ \mu) \tag{6.7}$$

$$h_1(p,\mu,n) \le 0 \tag{6.8}$$

$$h_2(p,\mu,n) = 0 \tag{6.9}$$

$$s_1(n) \le 0 \tag{6.10}$$

$$s_2(n) = 0 \tag{6.11}$$

$$p_k^{\mathrm{L}} \le p_k \le p_k^{\mathrm{U}} \quad \forall k \tag{6.12}$$

$$n_d^{\mathrm{L}} \leq n_d \leq n_d^{\mathrm{U}} \quad \forall d \tag{6.13}$$

$$\mu_w^{\mathrm{L}} \leq \mu_w \leq \mu_w^{\mathrm{U}} \tag{6.14}$$

Hereby, the objective function C describing the performance metric depends on the solvent's structural information n (e.g., a vector containing several groups when a GC method is employed), a set of estimated properties p, and the process variables μ. The molecular properties p are predicted using the model f as shown in eq. (6.7). General constraints are denoted by h, such as the process model, while structural constraints for feasible solvent structures are represented by s (e.g., valency). Upper and lower bounds, denoted by superscripts U and L, are given in eqs. (6.12)–(6.14), which limits each property in p, the size, structure, and/or the complexity of the solvent identifier n, and the process variables μ. The minimal value of the performance metric will be determined by choosing the optimal solvent identifier n accompanied by the optimal process conditions μ. This integration of solvent and process decision variables makes the optimization problem more complex than either a pure CAMD problem or a pure process optimization problem. Moreover, due to the solvent decision variables, the integrated problem usually contains integer variables, resulting in a challenging mixed-integer nonlinear problem (MINLP). Several solution frameworks have been proposed for this challenging optimization problem, whereby some approaches avoid such a mixed-integer formulation to obtain a less complicated nonlinear optimization problem (NLP).

General overviews of the field of integrated solvent-process design can be found in review articles discussing CAMD methodologies. Detailed reviews summarizing the state of the art in this field of research were published in the last few years [3, 69]. Shorter communications complete the overview articles with new developments addressing the field of integrated design directly [11, 99]. Hereby, Gertig et al. focus on CAMD methods based on quantum chemical approaches, especially discussing the solvent design for reactive systems and the design of catalyst structures [25]. Recently, the perspective of process systems engineering on material design in general, including CAMPD, was discussed by Adjiman et al. [1] in an overview article.

6.4.2 Survey of Integrated Solvent and Process Design Methodologies

The various frameworks for integrated solvent and process design can be classified into manifold categories. These categories may be, for example, the method used to solve the optimization problem, the thermodynamic prediction method, or the technical application considered in the case study. However, all of these categories are not fully selective, and, therefore, hybrid approaches that belong in more than one category can always be found. It should be noted that within the scope of this chapter,

only a selection of contributions to the field of integrated design can be presented, which are discussed in the following.

The idea of integrated solvent and process design emerged in the late 1990s. Pistikopoulos and Stefanis presented a solvent design methodology in which the overarching postulated goal was to minimize the environmental impact. To this end, a three-step framework was proposed consisting of identification of agent-based process operations, generation of suitable solvent candidates satisfying environmental and processing constraints, and verification on the process level to determine economic costs. The prediction of the molecular properties was done by use of GC methods, and the methodology was successfully applied to two gas adsorption tasks as case studies. Trade-offs between economic and ecological criteria were analyzed and discussed. The stepwise approach was evaluated as a suitable tool for reducing the combinatorial complexity, later denoted as the decomposition approach. Although the scope of this initial work was even more holistic, the general idea of CAMPD was born: predictive thermodynamics is used to evaluate a process so that the solvent selection is based on the process performance [71]. In follow-up work, this methodology was extended to design binary mixtures used as solvent systems [9].

On that ground, Hostrup and coworkers [33] proposed an integrated solvent and process design strategy for separation processes by combining heuristics and mathematical optimization. A superstructure of alternative separation technologies was suggested, which was reduced by the application of task specific constraints. Afterward, solvent candidates were generated for the remaining separation technologies. The final MINLP was solved by enumeration. Two case studies were presented. One was the generation of a flow sheet for the separation of an azeotropic mixture, and the other was a water treatment problem [33]. Marcoulaki et al. applied stochastic simulated annealing for the optimization and exemplified their method for liquid–liquid extraction, extractive distillation, retrofit design, and absorption processes [59]. Two years later, a multiobjective integrated solvent and process design were published determining Pareto optimal solutions. Environmental criteria and uncertainties were considered for the design of the solvents. The application, the recovery of acetic acid, was modeled and optimized using Aspen Plus [47]. Eden et al. [17] came up with a different solution strategy: The problem was reformulated into two reverse problems by decoupling the balance equations and constitutive equations. The resulting problem could be visualized and solved using a property clustering technique, which allowed the projection into a ternary diagram. The information from the property cluster diagram was used for a CAMD to identify solvents that correspond to the desired cluster values [17]. This strategy has been expanded to the use of GC methods for molecular design [18], and finally, for the identification of properties that provide optimal process performance [10]. Cheng and Wang [14] developed a two-stage computational scheme for the solution of integrated design problems. First, a feasible solution was determined using a

mixed-integer hybrid differential evolution algorithm, which is a genetic algorithm (GA) for the global optimization of MINLPs. Second, the identified feasible solution was numerically validated to be optimal using a quadratic programming algorithm. The approach was used to identify a biocompatible solvent for a fermentation–separation process for ethanol production consisting of a two-phase fermenter, an extractive distillation, and a distillation column for solvent recovery [14]. First et al. [20] dealt with an integrated material and process design by investigating a zeolite for the separation of methane and CO_2. Hereby, the architecture including shape, size, and pore selectivity was part of a screening step, followed by a process optimization to determine the costs. In order to make the partial differential algebraic equation system manageable in optimization, a Kriging surrogate model was developed to describe the pressure swing adsorption [20].

A broad framework, which was extended over many years, was developed by Papadopoulos et al. In a first contribution, a multiobjective CAMD method was presented to determine a Pareto-optimal set of molecules with respect to desired thermodynamic and/or environmental properties using GC methods such as UNIFAC. The Pareto optimal candidates were evaluated on the process level. Suboptimal decision-making due to the use of a single objective optimization was avoided at the cost of an increased number of process optimizations [65]. This drawback was tackled by introducing a property clustering approach in which one molecule was selected as representative for a cluster of molecules with similar properties in the Pareto set [66]. The framework was applied to liquid–liquid extraction, extractive distillation, and a gas adsorption process. A subsequent study investigated problems of industrial complexity involving reactive systems [67] workflow [68]. Since a dynamic model was not available, controllability was verified by calculating the variations of the steady state of the system due to small manipulations of some control variables. Besides the controllability assessment, a second process design stage for the most promising candidates was suggested using rigorous process models.

6.4.2.1 Approaches Using Alternative Thermodynamic Models

As an alternative to UNIFAC for describing activity coefficients, Keskes et al. [42] proposed the use of the SAFT-VR model for CO_2 capture from methane in a conference contribution, which was studied in detail afterward [42, 70]. Burger et al. [8] proposed a hierarchical framework using a GC method for SAFT-γ Mie. In the framework, reduced unit operation models were considered at the first stage and surrogate models were developed to estimating contributions to the objective function. The Pareto optimal candidates were defined via multiobjective optimization, and the detailed problem was solved for these candidates [8]. SAFT-γ Mie was also applied for the working fluid selection of an organic Rankine cycle process including transport properties [91]. Another thermodynamic model was used by Siougkrou

et al. [82]. GC-VTPR was applied to investigate a Diels–Alder reaction using experimental kinetic data considering three solvent candidates.

A novel methodological approach was proposed by Scheffczyk et al. using the method COSMO-RS in combination with pinch-based shortcut models [76]. The use of COMSO-RS eliminated the need for GC methods, thereby increasing the complexity of the molecules in the solvent design space. For the evaluation of the shortcut models, NRTL parameters were regressed using COSMO-RS generated activity coefficients for solvent mixtures with candidates that passed a prescreening step. In the case study, a databank of molecules was screened for a solvent with minimum energy for a hybrid extraction distillation process that reduces the minimum energy demand by 63%. This concept was further developed to generate new molecules using a GA that overcomes the limitations of employing a database as solvent design space [77]. Fleitmann et al. [21] applied this methodology to the CO production from CO_2 captured from natural gas. Hereby, a storage molecule was generated as an intermediate so that excess energy from renewable energy sources could be stored chemically [21]. Additionally, a second level for the process design was introduced that evaluates solvent candidates using rigorous process models.

6.4.2.2 Most Recent Contributions

Recently, a multistage design methodology for extractive distillation processes was proposed. It used a multiobjective CAMD method to identify Pareto-optimal candidates, followed by rigorous thermodynamic calculations and analysis using residue curves, and final process optimization [98]. Chen et al. [12] published an integrated ionic liquid and process design approach exemplified by azeotropic separation processes. UNIFAC-IL was applied to predict thermodynamics. Ten et al. [86] integrated safety and health aspects into the integrated design and applied the method to a gas adsorption problem. In terms of the prediction of reaction kinetics, Gertig et al. presented approaches to calculate kinetics using DFT and COSMO-RS to select the optimal reaction solvent or respectively catalyst based on process performance [24, 26]. Zhang et al. [93] also predicted reaction kinetics using DFT. However, the design objective was the identification of an optimal reaction solvent for an antioxidant [93]. Both contributions point to a novel direction in CAMPD.

6.4.2.3 Direct Optimization of Thermodynamic Parameters: Continuous Molecular Targeting

The continuous molecular targeting approach addresses the integrated solvent and process design optimization problem in a conceptually different way and is therefore presented in a separate section. Hereby, the parameters describing the solvent in the thermodynamic model are treated as optimization variables chosen by the optimizer. This means that the process is optimized together with the solvent parameters, resulting in an ideal reference case for a virtual solvent. A second step is

to search for real solvents that exhibit similar thermodynamic behavior to the virtual solvent. To this end, a Taylor approximation can be performed to evaluate the loss in the objective functions due to deviations from the optimal, virtual parameters. Alternatively, an integer-programming problem is solved using GC methods to design solvents having the same parameters as the virtual solvent as far as possible. Since this second step is a matching step for the thermodynamic parameters of the virtual solvent, the methodology requires a thermodynamic model in which the parameters are physically meaningful. The advantage of this technique is that the optimization needs to be performed only once and not repeatedly for all suitable solvent candidates. The price of this advantage is, of course, the increasing number of optimization variables and the verification of the validity of the matching decomposition step.

The continuous molecular targeting technique was first presented for the design of an adsorption solvent for carbon capture and storage [4, 5]. PC-SAFT was used as a thermodynamic model since it has a sound physical basis by considering repulsion, dispersion, association, and multipole interactions. Detailed information on this modeling approach is discussed in Section 3.1.1. The process flow sheet for the CO_2 adsorption took into account a high-pressure adsorption unit, a pressure valve with a subsequent flash unit for desorption, and a pump to close the solvent recycle connected to the adsorption unit. The objective function to be minimized was the amount of solvent makeup needed to compensate for solvent losses. For the mapping step, the Taylor approximation method was used and a database with PC-SAFT parameters was evaluated to find real-world solvents with minimal deviations from the optimal, virtual solvent. The method identified dimethyl sulfoxide as the solvent with the lowest predicted solvent loss, representing a reduction of more than factor 1,000 compared to the reference adsorption solvent methanol.

The general continuous molecular targeting framework has been refined in various ways over the last few years: The integrated working fluid and process design for an organic Rankine cycle was successfully investigated and the mapping using GC methods was introduced [53, 54]. Besides equilibrium thermodynamics, transport properties were included for the process design, and the potential of mixtures as working fluids instead of pure components was investigated [78, 80]. The approach was successfully applied to an antisolvent crystallization process using PC-SAFT and a convex hull method to reduce the solvent design space [89]. For the crystallization application and the organic Rankine cycle each, a superstructure optimization approach was developed using continuous molecular targeting [79, 90].

6.4.2.4 Integrated Solvent and Process Design for the Kinetics of Chemical Reactions

While solvent selection for reaction kinetics has already been considered in CAMD approaches [84], the first contribution for selecting a reaction solvent in a CAMPD was proposed by Zhou et al. [95] and is presented more in detail below. The approach aims at maximizing the total process profit, as is schematically shown in Figure 6.9. The prediction of reaction rates can be done on a theoretical basis by searching for the transition states and their QM calculation as presented in Sections 3.2.2.3 and 6.3. However, since these investigations are time consuming, a data-based approach was chosen for the integrated design: Experimentally determined reaction rates were fitted to a linear quantitative structure–property relationship (QSPR) model using quantum chemically based descriptors derived from σ-profiles. The σ-profile of a molecule is a histogram of the electric charges on the surface of the molecule, which is embedded in an ideal electrical conductor [51]. These σ-profile-based descriptors were derived by dividing the histogram into six sections and integrating each section resulting in six descriptors representing each solvent candidate. Eq. (6.15) shows the structure of the QSPR, where k denotes the reaction rate, S_i are the six descriptors, and a denotes the fit parameters. The model enabled the prediction of reaction rates in unknown solvent candidates by using the candidate's sigma profile:

$$\log(k) = a_0 + \sum_{i=1}^{6} a_i S_i \tag{6.15}$$

However, the σ-profiles must be available for all potential candidates. In general, this means that a geometry optimization and a single point energy calculation must be performed using the continuum solvation model COSMO [51]. Since the full σ-profile was not needed, but only the six descriptors representing sections of the profile, a GC method was established for predicting these six descriptors. Molecules were encoded into UNIFAC groups, and the contribution of each group to one of the sections was regressed using molecules with available σ-profiles. In this way, the time-consuming QM calculation could be avoided. In addition to predicting the reaction rate, GC models from the literature were taken to estimate the boiling point, critical point, enthalpy of vaporization, density, and heat capacity of the solvent candidates. This approach was applied to a Diels–Alder reaction evaluated on a simple process configuration including a CSTR, a distillation column, and a recycle of unreacted reactants and solvent. The best performing solvent in experiments, acetic acid, was outperformed by isopropanol, with a 20% increase in total process profit, highlighting the potential of integrated solvent and process design.

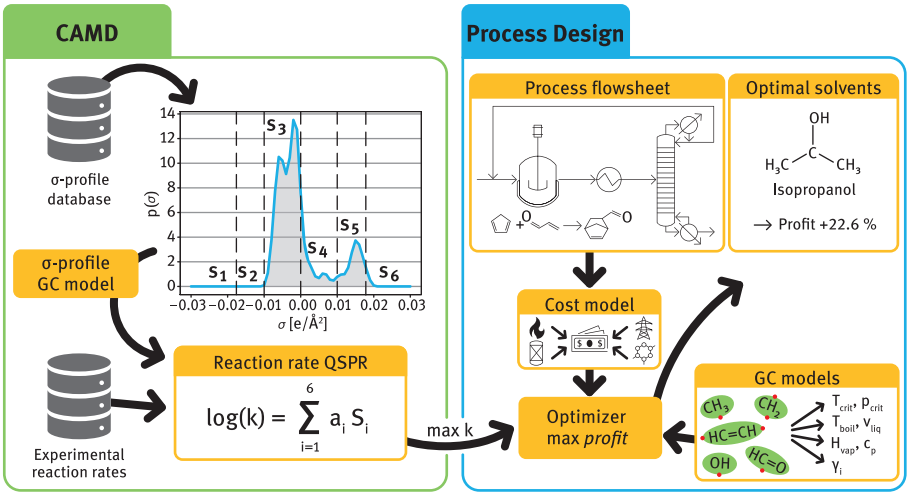

Figure 6.9: Overview of the reaction solvent design approach [95].

This selection approach was refined by applying a robust optimization method to account for uncertainties in the predictions [94]. The case study was adjusted to consider a competitive Diels–Alder reaction that distinguishes between the desired product and an undesired isomeric by-product. Consequently, two reaction constants k_1 and k_2 were regressed for the desired and the side reaction, respectively, to receive two QSPR models. The 14 parameters describing the two reactions were considered in a sensitivity analysis. Hereby, the 90% confidence interval of each parameter was taken separately without changing the other parameters, and it was sampled uniformly in this uncertainty region. For each sample point in these regions, the solvent leading to the highest reaction rate was computed. It was assumed that the most sensitive parameters would yield many different solvents with the highest reaction rate when the uncertainty region was sampled. It turned out that the fit parameters a_3 and a_4 for the side reaction are the most uncertain parameters according to eq. (6.15). Due to computational limitations, only these two parameters were included in the robust optimization framework. The objective of the robust optimization was to find the solvent that maximizes the average concentration difference between the desired and the side product over all scenarios considered. The final optimal solvent was the one that showed the largest concentration differences in most scenarios. The framework suggested new solvent candidates; however, since the first three most promising solvent candidates contain fluorine, the inclusion of HSE properties in the solvent design process were suggested for future work.

6.4.2.5 Genetic Optimization Approach for Complex Solvent-Process Optimization Problems

This inclusion of HSE criteria was one aspect in a CAMD approach for a reactive multiphase system exemplified by an extractive reaction, where biocompatibility was included as a constraint in the solvent design [96]. This study was a preliminary work, the results of which were used for an integrated design presented afterward. A new methodology was developed to calculate the combined reactive and liquid–liquid equilibrium simultaneously. To this end, the problem was treated as a system of ordinary differential equations (ODEs) describing a mass transfer problem within several phases. The ODEs were solved until the steady state was reached, indicating that the equilibrium compositions were achieved in all phases. This algorithm was shown to provide robust and efficient solutions for complex phase equilibria including equilibrium reactions and was an important achievement for the calculation of phase equilibria in the following integrated design works. Despite these achievements, the calculation of phase equilibria was still time-consuming in the context of optimization, therefore, a GA was applied for the solvent design step instead of solving the MINLP deterministically. Hereby, a set of solvent candidates is chosen as starting generation, their performance in the objective function is calculated, and the most efficient candidates are used with a higher probability for genetic operations. In this context, genetic operations were alterations of the structure of the molecules, such as the replacement of a group in a molecule or the creation of a new molecule from two existing ones. To perform these operations easily, the molecules had to be encoded flexibly. In the proposed method, molecules were represented as a tree graph. UNIFAC structural groups served as nodes of the tree and were connected to form molecules with physically feasible structures. In the case study, the GA showed its ability to design suitable molecules that maximize the equilibrium conversion of the reactant.

Since these achievements were encouraging in the CAMD, the methods were applied in an integrated solvent and process design as well. The objective was to develop a solvent for a coupled adsorption–desorption process to remove acetone from the air [97]. For each solvent generated by the GA, the NLP describing the process conditions was solved. Using this hybrid solution strategy enabled the solution of such a complex optimization problem, which was practically not possible with state-of-the-art MINLP solvers like branch-and-reduce optimization navigator (BARON). This hybrid framework is schematically shown in Figure 6.10.

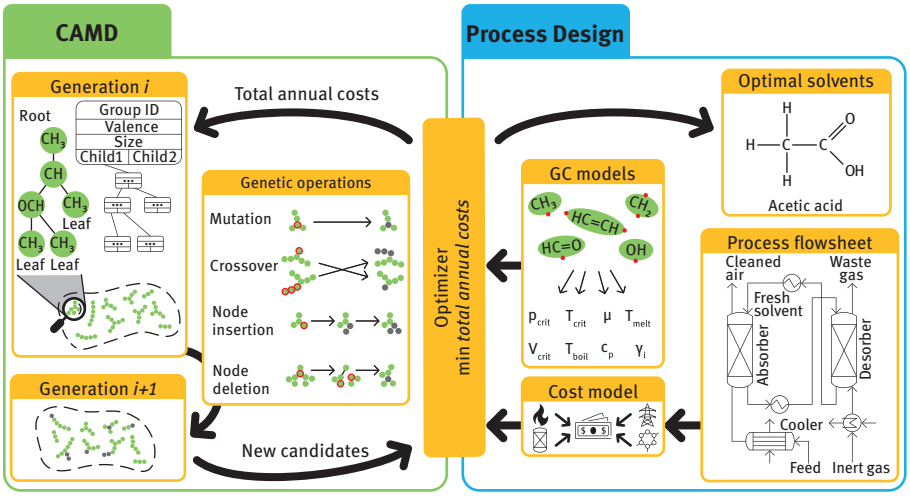

Figure 6.10: Hybrid stochastic-deterministic optimization approach for an integrated solvent and process design [97].

6.4.3 Integrated Solvent and Process Design for Thermomorphic Multiphase Systems

While the works described above are dedicated to the design of single molecular components, McBride et al. [60] studied the potential to design novel multicomponent TMS. The hydroformylation of long-chain alkenes was considered as reaction example of practical relevance. The design methodology is based on COSMO-RS since a predictive thermodynamic model for the catalyst–ligand complex of rhodium and BIPHEPHOS was needed. A database approach of successive screening steps was proposed to identify promising catalyst carrier solvents and product extraction agents before these candidates were composed to multicomponent solvent systems. The results confirmed that the state-of-the-art TMS, consisting of dimethylformamide (DMF) and *n*-decane was very efficient from a thermodynamic point of view and was predicted to outperform other TMS. Consequently, a process optimization scheme was set up for the hydroformylation using the DMF-based TMS [61]. Since the cost caused by the leaching of the catalyst complex was included in the objective function, a multistage extraction cascade with solvent regeneration by distillation was considered. The investigation revealed that the optimal number of extraction stages is five. In particular, it was found that a classical TMS-based process with only a single decanter is significantly inferior, making such a process design economically infeasible. This finding opened the door for further solvent-based considerations, as DMF is on the list of very high concerns of the REACH legislative for being developmental toxic, and thus should be replaced. When multistage extraction is unavoidable, solvents with

lower extraction power but “green” properties, that is, appropriate HSE properties, can be used if an increased number of extraction stages is used to compensate for the lower extraction power.

For this purpose, a refined solvent screening was established considering HSE criteria such as fish toxicity, carcinogenicity, or flash point. These properties were predicted using QSPR models published in the literature and are also applied in authorization processes for novel chemical compounds under REACH [6, 87]. By evaluating these models, potential solvents could be excluded from the candidate list. Preliminary results of this procedure were published, and the most promising solvent candidates were successfully experimentally validated [62]. The final methodology involved 15 different green properties predicted by more than 30 different models. Besides that, the methodology included conformers, was completely automated, and databases for the prediction results were established so that fast relaxations of the green screening criteria could be made and examined [56]. Hereby, diethylsulfoxide (DESO) was identified as a particularly efficient replacement candidate for DMF, as it showed a remarkably similar thermodynamic behavior. The identified candidates were used below for an integrated solvent and process design, as shown later.

First, systematic process optimization was performed for the candidates identified in the preliminary screening study, namely dimethylsuccinate (DMSU), tetrahydropyranone (THPO), and, for reference purposes, DMF, which are all shown in Table 6.7 [43]. The process flow sheet is shown in Figure 6.11 along with the overall approach. The sequence of screening and process design can be seen as strong decomposition, but the restriction to three solvents offered the chance for rigorous process optimization. The main contribution of this study was the automated generation of surrogate models to efficiently perform the process optimizations for the different solvents. To this purpose, the techniques presented in Section 5.3.2 were applied. In order to efficiently calculate the liquid–liquid equilibrium and the partition of the catalyst in the decanter, the surrogate model technique of reduced dimensionality was used [48]. Next, a surrogate model for the solvent regeneration by distillation was developed that computes the costs directly from the feed composition [44]. The resulting set of equations was solved using the multistart local optimization of BARON to determine the optimal process cost. The analysis of the different processes revealed that THPO can compete with DMF within the uncertainty range of the economic objective function, while DMSU was less efficient due to its reduced catalyst extraction power. Therefore, THPO was successfully identified as a green alternative solvent with sufficient efficiency.

However, when this approach is applied, the solvent design space is limited to molecules available in the screening database. To overcome this limitation, a novel strategy for the integrated solvent design was introduced to expand the solvent design space to a region around promising solvents from the screening using QM-based descriptors. In a preliminary study, a CAMD problem was formulated using a

Table 6.7: Successfully identified solvent candidates by the screening of McBride et al. [62], which served as a candidate pool for rigorous process optimization [43].

Name (abbreviation)	Structure
Dimethylsuccinate (DMSU)	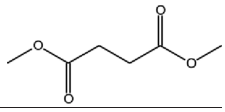
Tetrahydropyranone (THPO)	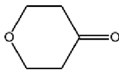
Dimethylformamide (DMF)	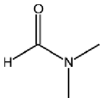

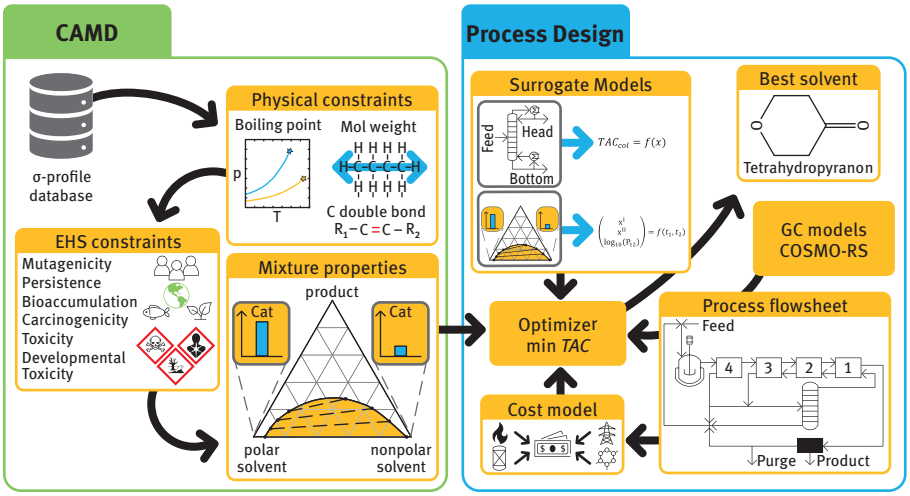

Figure 6.11: Integrated solvent and process design strategy for homogeneously catalyzed reactions using a decomposition consisted of a solvent screening for the molecular design and subsequent process optimization.

GC method to predict σ-profiles and two green properties, while the conductor-like screening model segment activity coefficient (COSMO-SAC) was applied to predict equilibrium thermodynamics [45]. The goal was to generate green solvent candidates that form a liquid–liquid equilibrium in the post-reaction mixture of hydroformylation and separate the catalyst. In a first step, solvents with low boiling points and appropriate green properties were generated by minimizing a weighted sum of the boiling point, the permissible exposure limit, and oral rat toxicity. Hereby, 20

candidates were identified. Secondly, these candidates were evaluated by maximizing the difference of the molar amount of the catalyst in the coexisting liquid phases.

This design approach yielded feasible green solvents suitable for catalyst separation and was therefore extended to an integrated design approach [46] as shown in Figure 6.12. A set of 17 promising solvents was determined by the final screening approach. On the one hand, the σ-profiles $h(\sigma)$ of these candidates were analyzed based on their first, second, and third σ-moments, which are the kth moments known from statistics and defined as $M^k = \int \sigma^k \cdot h(\sigma)\ d\sigma$. On the other hand, a moment for the ability of a solvent to act as acceptor for hydrogen bonding was chosen as characteristic: $M_{\text{acc}} = \int h(\sigma)\ f_{\text{acc}}(\sigma)\ d\sigma$, where f_{acc} describes the part of the σ-profile where the charge σ is larger than the threshold value σ'_{hb} of 0.01 e Å^{-1}. Interestingly, these moments laid in distinct domains or bands for the solvent candidates from the screening, except from two outliers. It was concluded that other relevant solvent candidates, which were not included in the solvent design space of the screening, will also lay in these bands. Therefore, a solvent design was introduced, and only the solvents whose σ-moments were in the target domain were considered in process design. The CAMD problem to generate solvents within the desired σ-bands was solved using a GC method for σ-profiles [57] and a set of appropriate molecular feasibility constraints [15, 74]. It should be noted that numerous candidates of the screening were not included in the solvent design space since only groups containing hydrogen, carbon, and oxygen were considered. This reduction was made under the assumption that molecules from these elements tend to be less hazardous. At the same time, the number of candidates was lowered decisively. Six suitable molecules were obtained from the CAMD problem solution and evaluated at the process level. The process configuration remained unchanged as shown in Figure 6.11, and again the process conditions were solved using the multistart local optimization option provided by BARON.

For four of the solvent candidates, feasible process operation conditions were found that meet all constraints in terms of molar flow rates, reactor model validity, and so on. Table 6.8 shows these four candidates, of which EMM and DMG outperform the reference solvent DMF regarding the total annualized costs. It is particularly encouraging that DMG is already known as a harmless solvent in the cosmetic industry, which proves its general suitability as a solvent. In total, this integrated solvent and process design approach showed its potential to identify new solvent candidates and to overcome the problem of a limited solvent design space if suitable databases are involved.

In conclusion, various approaches ranging from screening to CAMPD can be used for TMS design. The screening-based methodologies often can provide very valuable input for the optimization-based methods. It is important to note that different methodologies often lead to different solvent candidates for the same process.

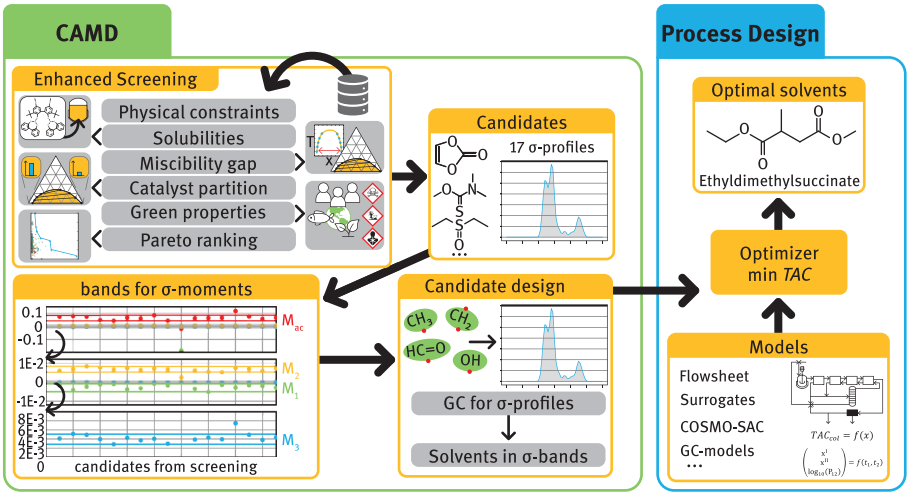

Figure 6.12: σ-Bands approach for integrated solvent and process design. First, a screening procedure identifies promising molecular structures. The σ-moments of these solvents are used to define general target domains for newly created solvents using a group contribution method. The final generated candidates are evaluated at the process level to determine their economic performance [46].

Table 6.8: Final solvent candidates identified by the integrated solvent and process design approach according to Figure 6.12 and proposed by Keßler et al. [46].

Name (abbreviation)	Structure	Name (abbreviation)	Structure
1-Ethyl 4-methyl 2-methylsuccinate (EMM)	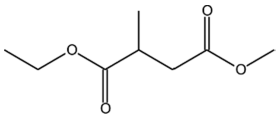	Ethyl levulinate (ELL)	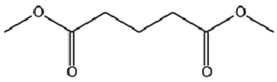
Dimethyl glutarate (DMG)	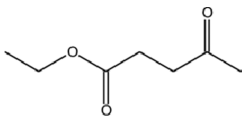	Methyl 2-ethylacetoacetate (MEA)	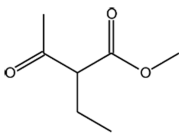

This is due to different solvent design spaces considered, different strictness of HSE criteria applied, different thermodynamic models used, and/or different decision criteria applied for ranking the candidates. Concerning the latter decision-making aspect, CAMPD has clear advantages over screening approaches since trade-offs between different thermodynamic properties are rationally made on cost. However, evaluation on the process level requires some effort and can be tedious. For the hydroformylation example discussed here, numerous candidates of the screening were not included in

the solvent design space of the σ-band-based CAMPD (Figure 6.12), which explains the appearance of different candidates. However, from a physical point of view, the results obtained from the different methods point in a similar direction, namely that mid-polar solvents are best suited as catalyst carriers. To answer the question, which of all molecules proposed is finally the best, it must be noted that such a rigorous answer cannot be given in terms of green solvents since the weighing of green properties is, inherently, highly subjective. For example, a rational, clear trade-off between fish toxicity and carcinogenicity is not possible. Such decisions must be made based on legal regulations and company policy, but also depend on the opinion of the individuals taking decisions. In terms of economy, the identification of an optimal solvent is clearer because all decisions can be finally boiled down to cost. The next step in this identification is the reduction of uncertainty for promising solvent candidates. Experimental data, in particular on the kinetics of a reaction to be performed in these solvents and the phase equilibria of the most important separation steps in the process, must be collected. The experiments will also reveal whether unforeseen complications may arise, such as unwanted reactions of the candidate solvent, or, related to a TMS process, the formation of an emulsion under separation conditions, either of which would result in the rejection of the candidate. However, the candidates evaluated successfully in experiments can subsequently be compared in a more detailed process optimization study based on the data obtained, so that the best candidate can be selected on a secure knowledge base. Generally, CAMD/CAMPD methods are not recommended to be used for final decision making of a solvent, but for isolating a manageable set of very promising candidates which then should be assessed in detail experimentally.

6.4.4 Conclusions

The concept of integrated solvent and process design is known for its potential to find novel solvents that are more efficient by making decisions based on process performance. This approach helps to avoid wrong decisions in solvent selection since all complex, hidden interactions at the process level are considered – at least within the assumptions and simplifications made. Since the optimization problems involved in combined solvent-process design decisions are very challenging to solve, various solution strategies and frameworks can be found in the literature. Different approaches tackling the same task may lead to different solvent candidates due to different design spaces, constraints, optimization algorithms, decompositions steps, or because of uncertainties in the thermodynamic prediction methods. Finally, experimental validation is required due to these uncertainties and possible unforeseen chemical effects.

Overall, integrated solvent and process design are in line with the trend to consider molecular DoF in the design of chemical processes. The levels from molecule to process addressed in Section 6.1 are more strongly interwoven to overcome the

classical heuristic-hierarchical design approach. Despite significant progress of computer-aided solvent-process design, carefully collected and evaluated experimental data remain an indispensable element for designing a final process at the lowest possible uncertainty. Where measurements need to be made and how the increasing experimental knowledge should be embedded in the final process design, is discussed in Section 6.5.

6.5 Integrated Model-Based Process Design Methodology

Stefanie Kaiser, Karsten H. G. Rätze, Fabian Huxoll, Gabriele Sadowski, Kai Sundmacher, Sebastian Engell

The computer-aided solvent selection and process design approach presented in Section 6.4 represents one possible formulation of the algorithmic part of caPSS (Section 6.2, Figure 6.3). Nevertheless, it is based on the assumption that the phase system and the process structure have been selected before and reliable information on thermodynamics and kinetics is available. In reality, however, this is part of an iterative selection and design process in which there is significant uncertainty about the quantitative description of the underlying phenomena. In this section, we discuss the interaction between algorithms and process developers including experimental work that is done to reduce the model uncertainties. This builds on the computer-based tools that are described in Chapter 5. Due to the complex nature and the multitude of viable approaches to the realization of each block in the caPSS framework, this section can only discuss a limited set of options for integrated design approaches.

One of the most important integration steps in the caPSS framework concerns the combination of experimental work with model-based process synthesis (Section 5.3). Model-based procedures require a thorough understanding of the underlying thermodynamics (Section 3.1), knowledge about the reaction networks and kinetics (Section 3.2), insight into the mass transfer mechanisms (Section 3.3) as well as experience in the development and operation of chemical production processes (Chapter 4). Therefore, this integration exemplifies the combination of different sources of knowledge in the integrated design of multiphase chemical processes.

Instead of assuming the availability of accurate models of the thermodynamics, reaction kinetics, mass transfer coefficients, and separation efficiencies at the beginning of the process design workflow, an additional loop is added to the caPSS framework in which suitable models are identified and calibrated iteratively during the evaluation of the final process design in terms of reaction and separation performance, sustainability and economic potential (Section 6.2.4). This iterative process contains the repeated creation of intermediate process design candidates based on all information that is available at this point in time but taking into account the model uncertainties. To reduce

the uncertainty, mbOED is integrated into the design procedure to improve the available data efficiently via systematic and carefully selected experiments.

After a short introduction to experimental design and, in particular, mbOED, the integrated process design in which process designs under uncertainty and experimental design are combined is presented. Then, approaches to the integration of additional tools which are described in Chapter 5 are introduced and discussed.

6.5.1 Experimental Design for Efficient and Accurate Parameter Identification

One crucial aspect in integrated process design is the bridge between fundamental knowledge and its utilization in process development in the form of mathematical models as shown in Figure 6.13. These models not only have to accurately represent the physicochemical phenomena but also require a form and implementation which keeps the computational load in simulation and optimization to a minimum. If the general structure of a model is fixed, either based on first-principles or via surrogate approximations, the identification of the associated model parameters using experimental data is required. Due to significant efforts in terms of time, manpower, and money that are necessary to generate such data, the generation of data that is most useful with respect to the design decisions is desired.

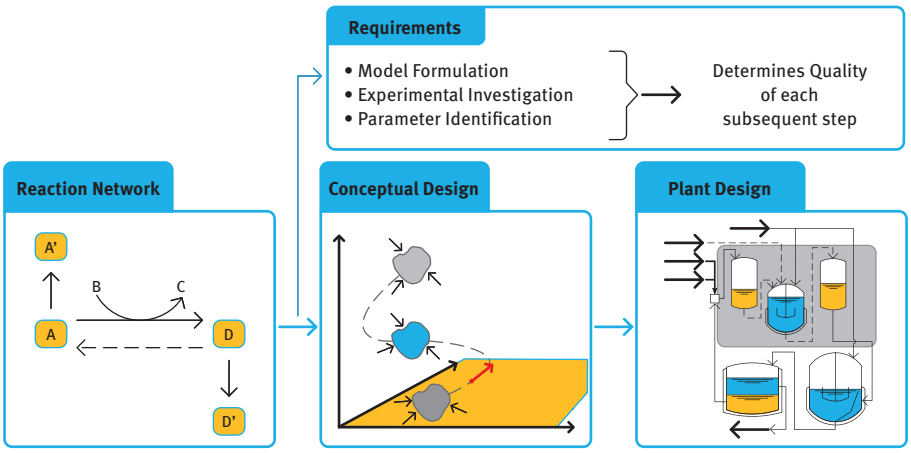

Figure 6.13: Schematic representation of the process development procedure for chemical production plants. Conceptual design: Figure 5.34 adopted from [85]. Plant design: Adopted from [72].

Experimental design approaches encompass heuristics, statistical design of experiments (DoE) and mbOED. For better differentiation, Figure 6.14 provides a schematic representation of the different design approaches. Whereas heuristics, in

particular the "one-factor-at-a-time" (OFAT) approach, are not well suited for parameter identification for nonlinear models, statistical designs like factorial or Latin hypercube designs as well as tailor-made mbOED approaches are able to capture nonlinear process behavior and multifactor interactions [88]. Especially, mbOED is subject to active research because of its wide applicability in model discrimination and parameter identification [32] via the design of sequential and/or simultaneous, potentially dynamic, experiments [22]. For parameter identification, mbOED is usually based on the Fisher information matrix (FIM)

$$F_\theta = F_{\theta,\text{prior}} + \sum_{j=1}^{n_{\text{Exp}}} \sum_{i=1}^{n_{\text{sp}}} \left(\frac{dy_{j,i}}{d\theta}\bigg|_{\theta^*} \right)^\top \sum_y^{-1} \frac{dy_{j,i}}{d\theta}\bigg|_{\theta^*}, \tag{6.16}$$

with the sensitivities $dy_{j,i}/d\theta \in \mathscr{R}^{n_y \times n_\theta}$ denoting the derivative of the measured variables y of experiment j and sampling point i with respect to the uncertain parameters θ. Here, all lowercase variables represent vectors while all uppercase variables denote matrices. In nonlinear process models, these sensitivity matrices may depend on the parameters so that they should be evaluated at the true parameter values θ^*. Since the true parameter values are usually unknown, they can be approximated by the current best guess $\hat{\theta}$. Eq. (6.16) also contains the measurement variance–covariance matrix Σ_y and available prior information $F_{\theta,\text{prior}}$. The inverse of the FIM F_θ^{-1} defines a confidence hyperellipsoid and provides an approximation of the nonlinear parameter confidence region. According to the Cramér–Rao lower bound, this confidence ellipsoid presents a lower bound to the true confidence region Σ_θ [58].

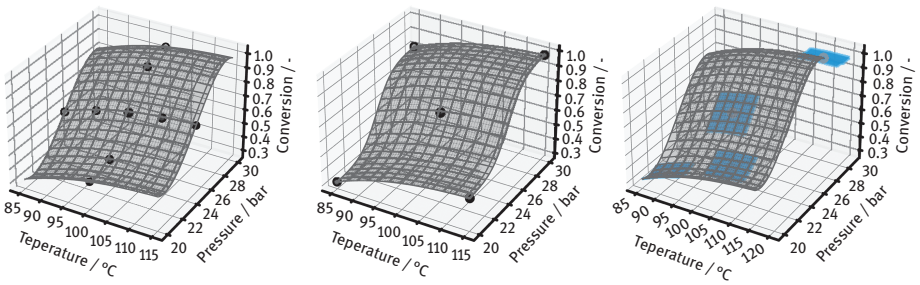

Figure 6.14: Schematic representation of the OFAT approach (left), factorial design with center point experiments (middle), and mbOED (right) for an exemplary two-factor (T, p) system. While the OFAT and factorial design provide a-priori schemata for optimally sampling the decision space, mbOED uses derivative information of the model output with respect to the parameters for a local approximation of the response surface (blue) to identify a sampling point with high sensitivity and decorrelating properties.

With this representation of the resulting parameter uncertainty, an optimization problem can be formulated as

$$\min_{u_1,\, u_2, \ldots,\, u_{n_{\text{exp}}}} \phi(F_\theta)$$

$$\left.\begin{array}{c} \text{Process model,} \\ \text{FIM definition: eq. (6.16),} \\ \text{Variational equations,} \\ \text{Path constraints,} \\ x \in \mathcal{X}, \\ u \in \mathcal{U} \end{array}\right\} 1, 2, \ldots, n_{\text{Exp}} \tag{6.17}$$

where a scalar metric of the FIM is minimized. In this formulation, the simultaneous design of n_{Exp} experiments are assumed with static control vectors $u_j \in \mathcal{U}$. The states $x_j \in \mathcal{X}$ may be constrained via additional path constraints and represent the solution to the process model while the sensitivity matrices in eq. (6.16) follow the variational equations.

In mbOED, various metrics ϕ are commonly used to scalarize the FIM. The most prominent of these are summarized in Table 6.9. In order to focus the experiments to identify specific parameters, weights can be introduced into the FIM yielding the modified FIM [73]:

$$\tilde{F}_\theta = W^{\frac{1}{2}} F_\theta W^{\frac{1}{2}}, \tag{6.18}$$

The combination of mbOED according to eq. (6.17) and process design via superstructure optimization will be discussed in the following.

Table 6.9: Subset of FIM optimality criteria for experiment design [22].

Criterion	Definition
A	$\phi(F_\theta) = \text{trace}\left(F_\theta^{-1}\right)/n_\theta$
D	$\phi(F_\theta) = \det\left(F_\theta^{-1}\right)^{1/n_\theta}$
E	$\phi(F_\theta) = \max\left(\text{eig}\left(F_\theta^{-1}\right)\right)$

6.5.2 Integrated Process Design

In the early stage design of new chemical processes, the most cost influencing decisions are taken, which makes it a crucial phase of process development. The pressure to reduce the development time is increasing due to shorter product cycles in the chemical industry and hence new strategies for fast, efficient, and risk-aware process development are needed. The established methodologies for process design can be classified into hierarchical or knowledge-based methods and optimization-

based methods. In knowledge-based process design, the design problem is divided into smaller subproblems which are then solved by the use of expert knowledge as introduced by Douglas [16]. Although the use of knowledge-based methods is still common in the process industries, it may fall short in terms of finding synergies between the different process units.

Optimization-based methods on the other hand find the optimal process configuration by solving an optimization problem [13]. The setup of this optimization problem however requires reliable process models. These models rely on experimental data to identify model parameters and physical properties. Sequentially performing laboratory experiments, identifying all model parameters and physical properties, and simulating and optimizing the process leads to long development cycles. To speed up the development and to reduce the experimental effort, a new methodology is proposed that integrates these steps.

Only a few works have been reported that focus on the integration of model identification and process simulation of optimization. Asprion et al. [2] integrated optimal experimental design in a flow sheet simulator. However, the framework focuses on model improvement and a good parameter estimation only and does not include a process design method. Marquardt and coworkers [73] developed integration of process optimization and optimal DoEs. By weighting the FIM as shown in Equation 6.18 in the optimal experimental design, they focus the experiments on the relevant parameters. However, in their approach uncertainties in the process optimization are neglected.

In this section, we integrate superstructure optimization under uncertainties (Section 5.3.3) with sensitivity analysis and optimal DoEs. After describing the proposed methodology and the sensitivity analysis as part of the methodology, we apply it to two case studies. The first case study is the hydroaminomethylation of 1-decene. In this case study, we show the results of a superstructure optimization under uncertainties and use these results to design a new experiment that reduces the variation in the prediction of the production costs. In the second case study, the hydroformylation of 1-dodecene, we will expand the methodology by global sensitivity analysis and show the improvements that are possible compared to a design methodology that is not focused on the identification of the cost-driving parameters.

6.5.2.1 Methodology

When first experiments have been performed and the most important elements of the process, for example, the phase system and the catalyst system, have been identified, the integrated process design starts. A schematic representation of the proposed methodology is depicted in Figure 6.15.

Starting with the first screening experiments, kinetic and thermodynamic models are developed that in the beginning will have significant parametric uncertainties.

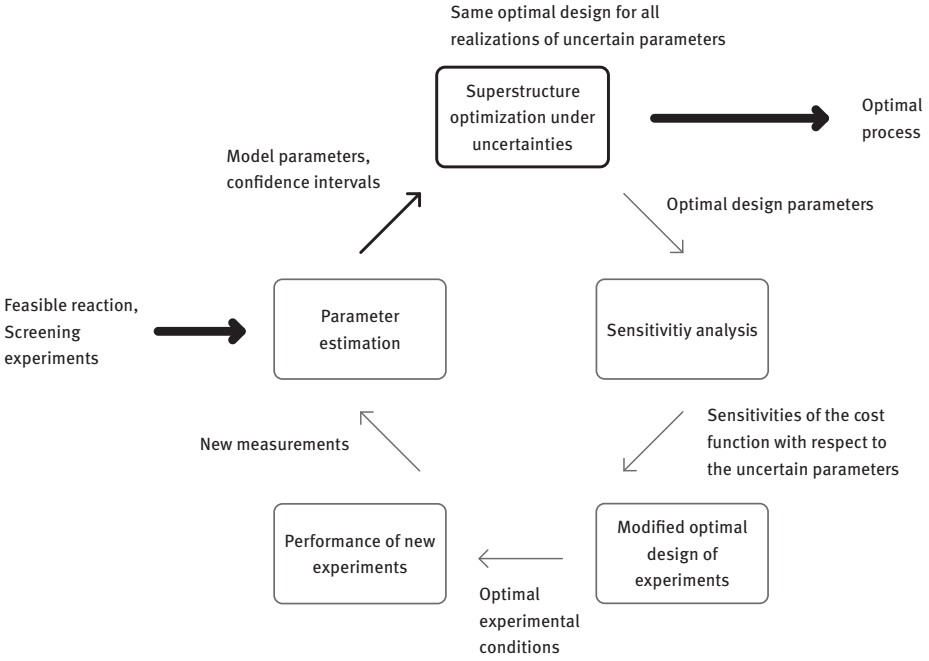

Figure 6.15: Schematic representation of the main elements of the integrated process design methodology.

These models are used in a subsequent step for superstructure optimization under uncertainties as explained in Section 5.3.3. At this point, it is checked if one or few process alternatives can be already identified as optimal. This would be the case if for all realizations the value of the cost function is lower for one design or a few designs compared to all other design alternatives. For large parametric model uncertainties, this is rather unlikely to happen. If no design could be identified as optimal, a sensitivity analysis of the cost function with respect to the uncertain parameters is performed to identify the parameters that have the largest impact on the cost function which will be explained in Section 6.5.2.2. The computed sensitivities are used as weights in the optimal DoEs to plan experiments that are focused on the determination of the most cost-relevant parameters.

6.5.2.2 Methods for Sensitivity Analysis in Process Synthesis

As lab experiments are expensive, process engineers want to identify those uncertain parameters that contribute most to the cost function of interest, for example, the production cost. For this, methods of local or global sensitivity analysis can be used. Local methods are computationally less expensive but provide reliable information

only in a small range around the nominal values of the parameters. Global methods require more computational effort but provide information for the entire parameter space [75].

Local sensitivity analysis can be performed by linear regression. Here, n uncertain parameters x_i are correlated to the regressed value $\hat{Z}_j$:

$$\hat{Z}_j = \beta_0 + \sum_{i=1}^{n} \beta_i x_i \tag{6.19}$$

The intercept β_0 and the regression coefficients β_i are determined via the least squares method. To standardize the regression coefficients with 0 mean and a standard deviation of 1, the standardized regression coefficients (SRC) are computed for N samples as follows [27]:

$$\mathrm{SRC}_j = \frac{\beta_j \hat{s}_i}{\hat{s}} \tag{6.20}$$

with

$$\hat{s} = \left[\sum_{j}^{N} \frac{\left(Z_j - \bar{Z}\right)^2}{N-1} \right]^{1/2} \tag{6.21}$$

and

$$\hat{s}_i = \left[\sum_{j}^{N} \frac{\left(x_i - \bar{x}\right)^2}{N-1} \right]^{1/2} \tag{6.22}$$

Since the SRCs are independent of the regressor, they can be used to compare the effect of the parameters on the objective function. Large SRCs correspond to a large impact on the objective. The samples are generated via perturbation from their corresponding nominal value. Thus, a linear approximation of the objective function in this region is generated.

In global sensitivity analysis, samples are taken from the entire parameter space. The sampling points should be distributed evenly. For this, Latin hypercube sampling can be used which is explained in Section 5.2.3. According to Sobol [83], the effect of a single parameter x_i can be computed via

$$S_i = \frac{\mathrm{var}(y|x_i)}{\mathrm{var}(y)} \tag{6.23}$$

Here, $\mathrm{var}(y|x_i)$ is the conditional variance of the output y with respect to the ith parameter. $\mathrm{var}(y)$ is the general variance of y. The total effect, which takes additionally nonlinear and interaction effects into account, can be computed as

$$S_{T,i} = 1 - \frac{\mathrm{var}\left(y|x_{\sim i}\right)}{\mathrm{var}(y)} \tag{6.24}$$

where $\mathrm{var}\left(y|x_{\sim i}\right)$ is the conditional variance of y with respect to all parameters except parameter i.

6.5.2.3 Case Study I: Hydroaminomethylation of 1-Decene

The approach presented above is applied to the hydroaminomethylation of 1-dodecene in a TMS [40]. The process includes unit operations for the reaction, phase separation, and the removal of the byproduct, water. As hydroaminomethylation can be considered as the sequence of the steps of hydroformylation and reductive amination, the kinetic models described in Hentschel et al. [29] and Kirschtowski et al. [50] (Section 3.2) are combined in order to get a first structure of the kinetic model. The parameters were fitted to experimental data of the hydroaminomethylation in a solvent system of methanol and dodecane. 12 different batch experiments where the concentration profiles were measured over time were used for the initial parameter estimation.

For the prediction of the solubilities of the components of syngas in the reaction medium and the phase separation in the decanter, thermodynamic models are needed. The gas–liquid and the liquid–liquid equilibrium can be predicted with PC-SAFT. The required parameters for the syngas, the solvents, and the main components are available in Huxoll [34]. Since the equations of PC-SAFT have to be solved iteratively, it is not suitable to use them directly in optimization [64]. Therefore, artificial neural networks were trained to predict the concentrations of hydrogen and carbon monoxide in the liquid phase depending on the temperature, the partial pressures, and the solvent composition. For describing the liquid–liquid equilibrium, the distribution coefficients defined as $K_i = \dot{n}_{i,\,\mathrm{polar}} / \dot{n}_{i,\,\mathrm{feed}}$ are fitted by artificial neural networks with respect to the temperature and the composition of the inlet of the decanter. The removal of water is modeled by a membrane model, using a solution-diffusion model.

The objective of the superstructure optimization is the minimization of the production cost per ton of the long-chain amine. The prediction of the costs includes the costs of the raw materials, the investments, and the utilities. As it is assumed that the solvents can be recovered in a further separation step, they are not included in the cost function.

The uncertainties considered here are the pre-exponential factors $k_{0,i}$ and the activation energies $E_{A,i}$ of the kinetic model resulting in 31 uncertain parameters. 35 different combinations of the uncertain parameters within their 95% confidence regions are used in the superstructure optimization under uncertainties. As described in Section 5.3.3, a two-stage optimization is performed where the design parameters are the

same for each scenario and are optimized under the assumption that the operating parameters (called recourse variables) are adapted to the actual values of the parameters in each scenario by control or online optimization during operation. Here, the design decisions include the binary decisions if the reaction is performed as a tandem reaction, meaning that all reactants and the catalyst are added into one reactor for the hydroaminomethylation, or if the hydroformulation and the reductive amination are performed in two subsequent reaction steps. The second binary decision is the choice if the polar and the unipolar solvent are added to the reactor forming a TMS system or if the nonpolar solvent is added after the reaction for phase separation and catalyst recycling. The recourse variables are the temperatures and partial pressures in the reactor, the solvent ratio, the temperature in the decanter, and the catalyst concentration.

The results for the four best designs that are structurally different are shown in Figure 6.16.

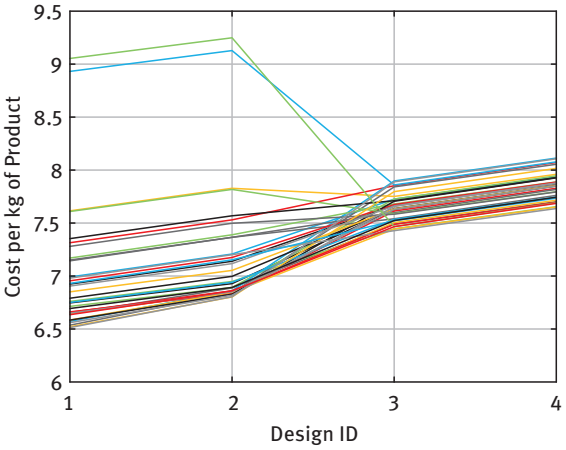

Figure 6.16: Costs for the four best process designs for different combinations of the uncertain parameters from the first superstructure optimization.

From Figure 6.16, it can be seen that no decision about the best design can be made at this point, which makes further model improvement necessary. The operating conditions can be adjusted depending on the realization of the uncertain parameters. The scaled operating conditions for design 1 are shown in Figure 6.17. It can be seen that the optimal operating conditions strongly depend on uncertain parameters.

The results of the sensitivity analysis after the first superstructure optimization that are presented in Figure 6.18 show that the reaction rate constants of the isomerization have the largest impact on the cost function. This can be explained by the fact that the reaction toward the side product *iso*-decene only occurs to a small extent and therefore this parameter is the most uncertain. The large variation of the side reaction leads to a large variation in the yield and hence in the production cost.

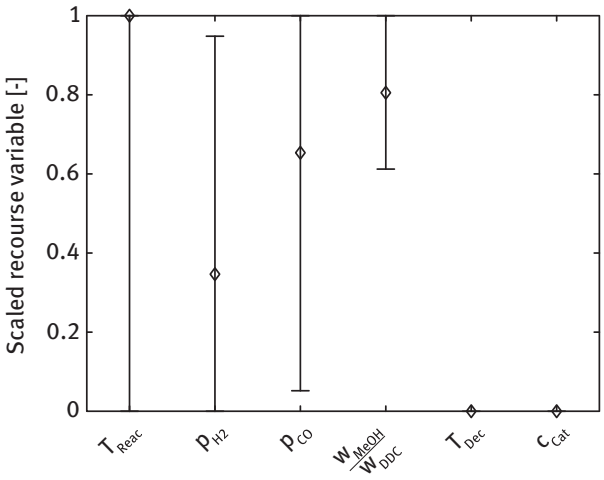

Figure 6.17: Recourse variables scaled with respect to their bounds.

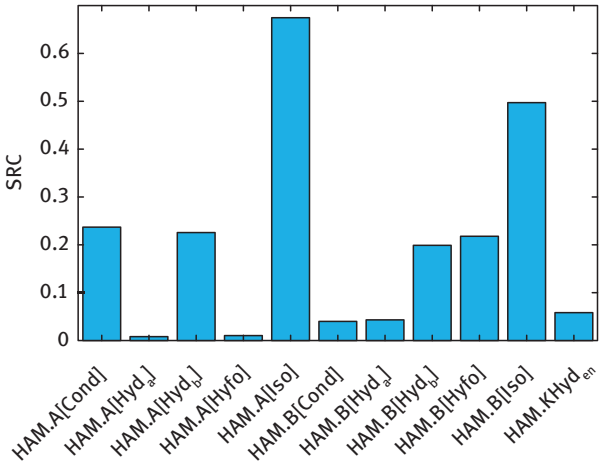

Figure 6.18: Standardized regression coefficients (SRC) for the kinetic parameters. Reproduced from [40].

The results of the weighted mbOED with the temperature, the pressure, the ratio of H_2 and CO, the catalyst concentration, and the sampling times as DoF are presented in Table 6.10. The optimal sampling times were identified as 6.5, 40.4, 40.4, 60, and 60 min.

The iterative process design is then applied using simulation experiments. The measurements are generated using a simulation model with the true parameters, corrupted by white noise with a standard deviation of 5%. In each iteration, the model parameters are updated using the new measurements, a superstructure optimization

Table 6.10: Optimally designed experiment for the hydroaminomethylation of 1-decene.

Temperature (K)	Pressure (bar)	Catalyst concentration ($mo_{Cat}/mol_{Substrate}$)	Gas composition (CO: H_2) (mol/mol)
136.4	50	0.002	0.5

is performed, the most relevant parameters are identified and a new experiment is planned. This procedure is repeated until one structurally different design is superior to the others for all discrete scenarios. For this desired result, eight additional experiments are needed if they are iteratively planned. The comparison of the iterative procedure and a model refinement using a full-factorial design with 16 additional experiments is shown in Figure 6.19. It can be seen that for the factorial design no decision about the best design can be made because the order is different for different scenarios although the number of experiments is twice as large as for the iterative procedure. Therefore, it can be concluded that the proposed model-based iterative process design can reduce the experimental effort and hence the time and costs for process development.

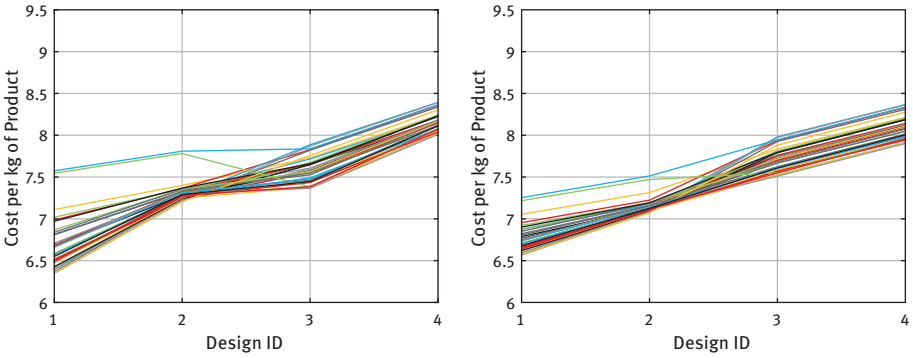

Figure 6.19: Comparison of the costs for the four best process designs for different combinations of the uncertain parameters after model refinement using 16 experiments planned by a full-factorial design on the left and after 8 iteratively designed experiments on the right.

6.5.2.4 Case Study II: Hydroformylation of 1-Dodecene

In this section, we show the benefits of using global sensitivity analysis in the integrated process development by applying it to the hydroformylation of 1-dodecene [41]. Here, we focus on the combination of sensitivity analysis and mbOED.

The process model that was used is described in detail by Hernandez et al. [30]. The pre-exponential factors and the activation energies of the hydroformylation and the isomerization of 1-dodecene of the kinetic model developed by Hentschel et al. [29]

are considered as uncertain parameters. All other parameters of the kinetic model have been observed as less influencing and are hence fixed to their predefined values.

In the mbOED, isothermal batch experiments are planned that measure the concentration profile over the batch time. The reaction temperature, the initial concentrations of 1-dodecene and *iso*-dodecene, the ratio of H_2 to CO, the catalyst concentration, and the sampling times of the concentration measurements are considered as DoF. The number of measurements taken during each batch experiment is fixed to six. The cost function is the yield of tridecanal in the product stream with respect to the 1-dodecene in the feed stream. Simulation results of a kinetic model with the true parameters, corrupted by white noise with a standard deviation of 5% are used as measurements of the batch experiments.

Three methods are compared: mbOED with unweighted FIM (normal), mbOED with the FIM weighted by local sensitivity analysis (local), and mbOED with the FIM weighted by global sensitivity analysis (global). For the first parameter estimation, the experiment is performed at two different temperatures and the measurements are taken equidistantly. In iterative steps of parameter estimation, mbOED, and a new experiment, planned according to the applied methods, a sequence of 25 new experiments was planned. The predicted yield over the number of experiments is evaluated and compared to a benchmark of a static factorial design where in total 32 experiments are performed at the lower and upper bounds of 5 DoF. In each iteration, the minimum and maximum yields are computed for the values of the uncertain parameters within the 95% confidence interval. To reduce the effect of random noise in the predictions, the mean values of 10 runs are considered. The evolution of the predicted yield is shown in Figure 6.20.

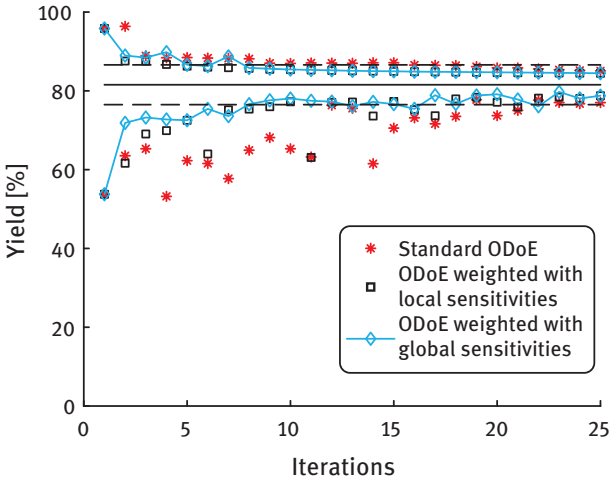

Figure 6.20: Evolution of the predicted intervals of the yield of tridecanal. The solid line represents the true yield and the dashed line represents the yield predicted with parameters obtained from a full factorial design of 32 experiments reproduced from [41].

The minimum and maximum predicted yields for all three cases are presented together with the true yield and the yield predicted using factorial sampling. After only 9 experiments, the prediction of the minimum yield is better compared to the factorial design in the case of the global sensitivity analysis and after 15 iterations in the case of the local sensitivity analysis. The standard mbOED performs erratically in comparison. This can be explained by the fact that in this case, it can happen that experiments are planned that improve a parameter with a low impact on the yield. It shows that by using weights on the parameters with a large impact on the cost function, more efficient experiments can be planned. As the global sensitivity analysis also takes nonlinear effects into account, it performs even better than the local sensitivity analysis.

It was shown how the integration of the DoEs and optimization under uncertainty can be used to accelerate the early design phase. Superstructure optimization under uncertainties helps to identify promising process alternatives and the variation of the predicted cost over the range of the uncertain parameters of a process design. Sensitivity analysis was applied to identify the model parameters that have a high impact on the final production costs. These parameters should then be determined by further experiments. An optimal DoE, in which the FIM is weighted by either local or global sensitivities, leads to fewer experiments that are required to reduce the variation in the cost function.

6.5.3 Advanced Integration Potential for Systematic Multiphase Process Design

The methodology presented in Section 6.4.2 can be extended to include further aspects in process design. Although only some applications were shown so far, the approach allows for many future applications. First, the integration in the methodology proposed for the selection of the phase system is possible. Simplified process models can be generated for each possible phase system and can be included in the superstructure optimization. As stated in Section 6.2, phase systems with the least possible number of additional substances are preferable. The two objectives – minimizing the process costs and using the least possible number of additional substances – can be evaluated by drawing the Pareto front, a curve of all results where one objective cannot be improved without worsening the other. Based on this evaluation, a decision about the best process can be made.

Moreover, methods for model-based solvent selection and optimal reactor design have been presented in Sections 6.3 and 5.3.1. As these methods are also part of the process design, the possibilities to include them in the integrated approach will be discussed in more detail in the following sections.

6.5.3.1 Model-Based Solvent Selection

Solvent selection is an important issue in the design of processes with liquid multiphase systems. Therefore, it is desirable to include solvent selection in the methodology for integrated process design. The proposed integration in the existing methodology is shown schematically in Figure 6.21.

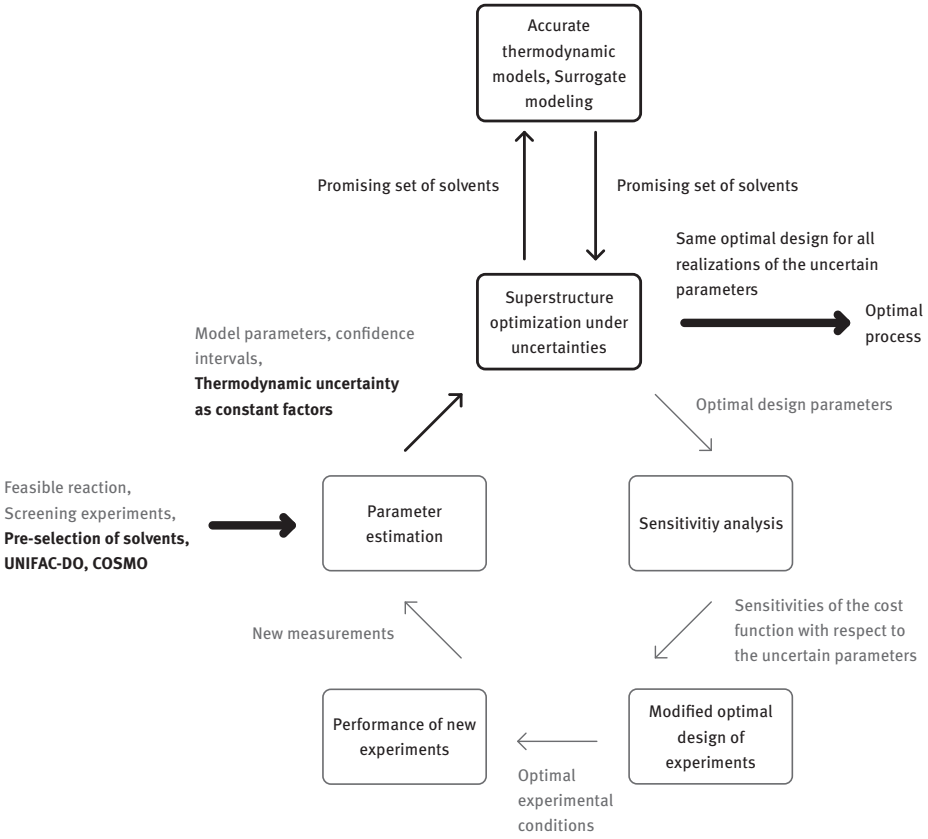

Figure 6.21: Proposed integration of solvent selection in process design. Blocks that are not part of the solvent selection procedure are marked in light gray.

The superstructure can be extended by thermodynamic models of all potential solvent candidates that have been selected based on expert's knowledge or by computer-aided solvent design as presented in Section 6.4. As the number of solvents that have to be considered might be large at this stage and accurate thermodynamic models will not be available for all of them, group contribution methods such as UNIFAC-Do can be used for a first approximation of the thermodynamic behavior (Section 6.3.3). Other options are, for example, the prediction by COSMO-RS as it was explained in Section 6.3.3.

The selection of solvents can be modeled in the superstructure optimization by binary variables, that is, one for each solvent. The maximum number of solvents that are allowed can be restricted using an inequality constraint. Constraints may have to be formulated to ensure that the desired behavior is reached. For example, the number of phases during reaction and separation can be predefined, for example, to ensure a single-phase reaction medium and a two-phase separation if a TMS system is used, as it was done in the case study presented in Section 6.5.2.3.

After a first superstructure optimization of the process, more detailed thermodynamic models can be derived for the most promising solvents. As described in Section 3.1, the application of PC-SAFT provides an accurate prediction of complex phase behavior, accounting for non-ideal interactions between the reactants/products and the solvents.

If such accurate models are not suitable for optimization, surrogate models as discussed in Section 5.2.3 can be applied. These models are used to replace the equations for the thermodynamic behavior in the process model. Following the methodology discussed in Section 6.4.2, the uncertainties in these thermodynamic models can then be reduced further until they do not influence the decision of the optimal process anymore.

This procedure enables not only to identify one optimal solvent but also to consider different numbers and combinations of solvents. Since the complete flow sheet is considered and optimized, it is possible to select a solvent system that provides the best overall performance.

6.5.3.2 Model-Based Optimal Reactor Design

While superstructure optimization in process design is able to identify the optimal interconnection and operation of elements from a set of preestablished, usually manually selected, unit operations, the EPF methodology from Section 5.3.1 represents an approach to the design of optimal reactor–(separator) networks without the necessity of a-priori knowledge about specific process units. This enables the identification of non-intuitive, non-standard reactor networks and operation strategies which might greatly improve the process performance.

While both approaches can be used for process development sequentially, a combination of superstructure optimization with the EPF methodology as one building block in the process design cycle represents a powerful addition to the integrated process design framework. Figure 6.22 contains a schematic representation of the interaction between mbOED and superstructure optimization including reactor network design via EPF. Two scenarios with different degrees of integration are possible.

Scenario 1: The flux-profile analysis (Section 5.3.1) is able to create reactor network candidates which need to be implemented and analyzed rigorously in terms of performance and cost [39]. Instead of manually comparing each of the reactor network candidates, these candidates can be used directly as unit operations in the

superstructure optimization. This integration enables the systematic evaluation of all candidates not only with respect to the reaction performance but also on the process scale, taking into account the downstream process (Figure 6.22).

Scenario 2: Instead of integrating reactor network candidates in the superstructure optimization, an "EPF reactor" with the extensions of axial dispersion, as discussed in Section 5.3.1, can be used as the sole reaction unit as shown by Hentschel et al. [28]. The simultaneous optimization of the operating conditions of the EPF reactor in the superstructure optimization replaces the inclusion of other reactor candidates which have fewer DoF and, therefore, show inferior performance. As a consequence, the superstructure is mainly used to identify the optimal downstream process and auxiliary process units. To incorporate the three-level approach to reactor network design of the EPF methodology, an additional iteration loop around the superstructure optimization is necessary to include realistic technical approximations.

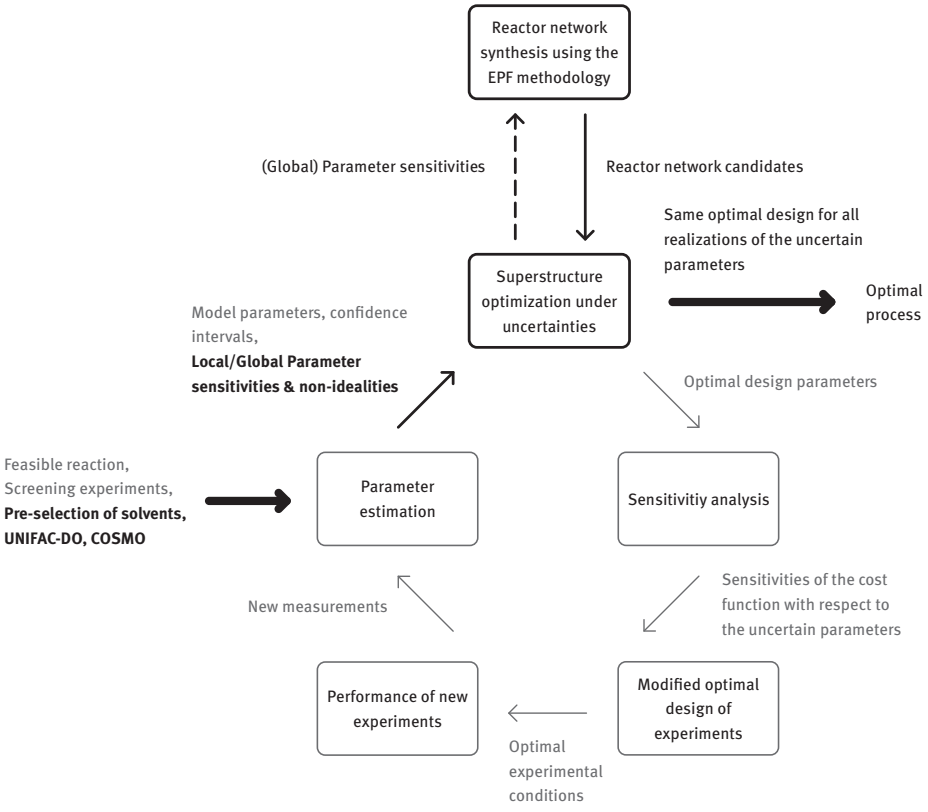

Figure 6.22: Integration of EPF-based reactor network candidates in the integrated process design framework. The interactions between superstructure optimization and EPF calculations are highlighted in dark gray. Global parameter sensitivities are only available in the second iteration cycle and therefore visualized with a dashed arrow.

The integration of the EPF methodology in this framework also enables synergistic effects. Consideration of uncertainty, especially parameter uncertainty, is of major importance in reactor design and leads to a more robust reactor and process performance. While Kaiser et al. [38] only considered the influence of uncertainty on the reactor performance, the combination of the probabilistic reactor design using sigma points with weights in the form of the global sensitivities with respect to the entire flow sheet allows for improved robustness of the process with optimally designed and operated reactor networks.

6.5.4 Summary

In this section, an integrated approach for model-based process development has been discussed. Model-based Optimal Experimental Design is a useful tool to identify model parameters with minimal experimental effort. However, usually, it does not focus on specific parameters, for example, parameters that are relevant for the uncertainty in the prediction of the final process costs. This can be overcome by using the integrated approach. By performing superstructure optimization under uncertainties, promising process designs can be identified and the impact of the model uncertainties on the production costs can be estimated via sensitivity analysis. Applying the computed sensitivities as weights in the mbOED enables focusing the experiments on the cost-relevant parameters to get a faster decrease of the parameter uncertainty. In this section, the application of this methodology was presented for two different processes, namely the hydroformylation of 1-dodecene and the hydroaminomethylation of 1-decene.

Finally, options for the extension of the methodology to further important aspects of the process development, for example, optimal solvent selection and optimal reactor design have been sketched briefly which are interesting fields for further research.

References

[1] Adjiman CS, Sahinidis NV, Vlachos DG, Bakshi B, Maravelias CT, Georgakis C. 2021: Process systems engineering perspective on the design of materials and molecules. Ind. Eng. Chem. Res. 60: 5194–5206.

[2] Asprion N, Böttcher R, Mairhofer J, Yliruka M, Höller J, Schwientek J, Vanaret C, Bortz M. 2019: Implementation and application of model-based design of experiments in a flowsheet simulator. J. Chem. Eng. Data. 65: 1135–1145.

[3] Austin ND, Sahinidis NV, Trahan DW. 2016: Computer-aided molecular design: An introduction and review of tools, applications, and solution techniques. Chem. Eng. Res. Des. 116: 2–26.

[4] Bardow A, Steur K, Gross J. 2009: A continuous targeting approach for integrated solvent and process design based on molecular thermodynamic models. 10th Intern. Symp. Proc. Sys. Eng. 813–818.
[5] Bardow A, Steur K, Gross J. 2010: Continuous-molecular targeting for integrated solvent and process design. Ind. Eng. Chem. Res. 49: 2834–2840.
[6] Benfenati E, Manganaro A, Gini G. 2013: VEGA-QSAR: AI inside a platform for predictive toxicology. CEUR Workshop Proceedings.
[7] Boz E, Tüzün NŞ, Stein M. 2018: Computational investigation of the control of the thermodynamics and microkinetics of the reductive amination reaction by solvent coordination and a co-catalyst. RSC Adv. 8: 36662–36674.
[8] Burger J, Papaioannou V, Gopinath S, Jackson G, Galindo A, Adjiman CS. 2015: A hierarchical method to integrated solvent and process design of physical CO2 absorption using the SAFT-γ Mie approach. AIChE J. 61: 3249–3269.
[9] Buxton A, Livingston AG, Pistikopoulos EN. 1999: Optimal design of solvent blends for environmental impact minimization. AIChE J. 45: 817–843.
[10] Chemmangattuvalappil NG, Eden MR. 2013: A novel methodology for property-based molecular design using multiple topological indices. Ind. Eng. Chem. Res. 52: 7090–7103.
[11] Chemmangattuvalappil NG. 2020: Development of solvent design methodologies using computer-aided molecular design tools. Curr.Op. Chem. Eng. 27: 51–59.
[12] Chen Y, Gani R, Kontogeorgis GM, Woodley JM. 2019: Integrated ionic liquid and process design involving azeotropic separation processes. Chem. Eng. Sci. 203: 402–414.
[13] Chen Q, Grossmann IE. 2017: Recent developments and challenges in optimization-based process synthesis. Ann. Rev. Chem. Biomol. Eng. 8: 249–283.
[14] Cheng HC, Wang FS. 2010: Computer-aided biocompatible solvent design for an integrated extractive fermentation–separation process. Chem. Eng. J. 162: 809–820.
[15] Churi N, Achenie LE. 1996: Novel mathematical programming model for computer aided molecular design. Ind. Eng. Chem. Res. 35: 3788–3794.
[16] Douglas JM. 1985: A hierarchical decision procedure for process synthesis. AIChE J. 31: 353–362.
[17] Eden MR, Jørgensen SB, Gani R, El-Halwagi MM. 2004: A novel framework for simultaneous separation process and product design. Chem. Eng. Proc. Proc. Intensif. 43: 595–608.
[18] Eljack FT, Eden MR, Kazantzi V, Qin X, El-Halwagi MM. 2007: Simultaneous process and molecular design – A property based approach. AIChE J. 53: 1232–1239.
[19] Ferro VR, Ruiz E, de Riva J, Palomar J. 2012: Introducing process simulation in ionic liquids design/selection for separation processes based on operational and economic criteria through the example of their regeneration. Separ. Purif. Techn. 97: 195–204.
[20] First EL, Hasan MM, Floudas CA. 2014: Discovery of novel zeolites for natural gas purification through combined material screening and process optimization. AIChE J. 60: 1767–1785.
[21] Fleitmann L, Scheffczyk J, Schäfer P, Jens C, Leonhard K, Bardow A. 2018: Integrated design of solvents in hybrid reaction-separation processes using COSMO-RS. Chem. Eng. Trans. 69: 599–564.
[22] Franceschini G, Macchietto S. 2008: Model-based design of experiments for parameter precision: State of the art. Chem. Eng. Sci. 63: 4846–4872.
[23] Gani R. 2019: Group contribution-based property estimation methods: Advances and perspectives. Curr. Opi. Chem. Eng. 23: 184–196.
[24] Gertig C, Fleitmann L, Schilling J, Leonhard K, Bardow A. 2020b: Rx-COSMO-CAMPD: Enhancing reactions by integrated computer-aided design of solvents and processes based on quantum chemistry. Chem. Ing. Tech. 92: 1489–1500.

[25] Gertig C, Leonhard K, Bardow A. 2020a: Computer-aided molecular and processes design based on quantum chemistry: Current status and future prospects. Curr. Opi. Chem. Eng. 27: 89–97.
[26] Gertig C, Fleitmann L, Hemprich C, Hense J, Bardow A, Leonhard K. 2021: CAT-COSMO-CAMPD: Integrated in silico design of catalysts and processes based on quantum chemistry. Comp. Chem. Eng. 153: 107438.
[27] Harrmann M. 2019. Contribution to the management of laboratory experiments in early phases of process development. Dissertation TU Dortmund.
[28] Hentschel B, Peschel A, Freund H, Sundmacher K. 2014: Simultaneous design of the optimal reaction and process concept for multiphase systems. Chem. Eng. Sci. 115: 69–87.
[29] Hentschel B, Kiedorf G, Gerlach M, Hamel C, Seidel-Morgenstern A, Freund H, Sundmacher K. 2015: Model-based identification and experimental validation of the optimal reaction route for the hydroformylation of 1-dodecene. Ind. Eng. Chem. Res. 54: 1755–1765.
[30] Hernandez R, Dreimann J, Vorholt A, Behr A, Engell S. 2018: Iterative real-time optimization scheme for optimal operation of chemical processes under uncertainty: Proof of concept in a miniplant. Ind. Eng. Chem. Res. 57: 8750–8770.
[31] Heyse A, Plikat C, Grün M, Delaval S, Ansorge-Schumacher M, Drews A. 2018: Impact of enzyme properties on drop size distribution and filtration of water-in-oil Pickering emulsions for application in continuous biocatalysis. Proc. Biochem. 72: 86–95.
[32] Hoang MD, Barz T, Merchan VA, Biegler LT, Arellano-Garcia H. 2013: Simultaneous solution approach to model-based experimental design. AIChE J. 59: 4169–4183.
[33] Hostrup M, Harper PM, Gani R. 1999: Design of environmentally benign processes: Integration of solvent design and separation process synthesis. Comp. Chem. Eng. 23: 1395–1414.
[34] Huxoll F, Jameel F, Bianga J, Seidensticker T, Stein M, Sadowski G, Vogt D. 2021: Solvent selection in homogeneous catalysis-optimization of kinetics and reaction performance. ACS Catal. 11: 590–594.
[35] Jameel F, Kohls E, Stein M. 2019: Mechanism and control of the palladium-catalyzed alkoxycarbonylation of oleochemicals from sustainable sources. Chem Cat Chem. 11: 4894–4906.
[36] Jameel F, Stein M. 2021: Solvent effects in hydroformylation of long-chain olefins. Mol. Cat. 503: 111429.
[37] Kaiser NM. 2019: Dynamic Optimization Based Reactor Synthesis and Design under Uncertainty for Liquid Multiphase Processes. Ph.D. Thesis. Otto-von-Guericke-Universität Magdeburg.
[38] Kaiser NM, Flassig RJ, Sundmacher K. 2016: Probabilistic reactor design in the framework of elementary process functions. Comp. Chem. Eng. 94: 45–59.
[39] Kaiser NM, Flassig RJ, Sundmacher K. 2017: Reactor-network synthesis via flux profile analysis. Chem. Eng. J. 335: 1018–1030.
[40] Kaiser S, Engell S. 2020: Integrating superstructure optimization under uncertainty and optimal experimental design in early stage process development. Comp. Aided Chem. Eng. 48: 799–804.
[41] Kaiser S, Menzel T, Engell S. 2021: Focusing experiments in the early phase process design by process optimization and global sensitivity analysis. Comp. Aided Chem. Eng. 50: 899–904.
[42] Keskes E, Adjiman CS, Galindo A, Jackson G. 2006: Integrating advanced thermodynamics and process and solvent design for gas separation. 16th Eur. Symp. on Comp. Aided Proc. Eng. and 9th Int. Symp. on Proc. Systems Eng. 743–748.

[43] Keßler T, Kunde C, Linke S, McBride K, Sundmacher K, Kienle A. 2019a: Systematic selection of green solvents and process optimization for the hydroformylation of long-chain olefines. Processes. 7: 882.
[44] Keßler T, Kunde C, McBride K, Mertens N, Michaels D, Sundmacher K, Kienle A. 2019b: Global optimization of distillation columns using explicit and implicit surrogate models. Chem. Eng. Sci. 197: 235–245.
[45] Keßler T, Kunde C, Linke S, McBride K, Sundmacher K, Kienle A. 2020: Computer aided molecular design of green solvents for the hydroformylation of long-chain olefines. 30th Eur. Symp. Comp. Aided Chem. Eng. 745–750.
[46] Keßler T, Kunde C, Linke S, Sundmacher K, Kienle A. 2022: Integrated computer-aided molecular and process design: Green solvents for the hydroformylation of long-chain olefines. Chem. Eng. Sci. 249: 117243.
[47] Kim KJ, Diwekar UM. 2002: Integrated solvent selection and recycling for continuous processes. Ind. Eng. Chem. Res. 41: 4479–4488.
[48] Kunde C, Keßler T, Linke S, McBride K, Sundmacher K, Kienle A. 2019: Surrogate modeling for liquid–liquid equilibria using a parameterization of the binodal curve. Processes. 7: 753.
[49] Kirschtowski S, Jameel F, Stein M, Seidel-Morgenstern A, Hamel C. 2021: Kinetics of the reductive amination of 1-undecanal in thermomorphic multicomponent system. Chem. Eng. Sci. 230: 116187.
[50] Kirschtowski S, Kadar C, Seidel-Morgenstern A, Hamel C. 2020: Kinetic modeling of rhodium-catalyzed reductive amination of undecanal in different solvent systems. Chem. Ing. Tech. 92: 582–588.
[51] Klamt A, Jonas V, Bürger T, Lohrenz JC. 1998: Refinement and parametrization of COSMO-RS. J. Phys. Chem. A. 102: 5074–5085.
[52] Klamt A, Schüürmann G. 1993: COSMO: A new approach to dielectric screening in solvents with explicit expressions for the screening energy and its gradient. J. Chem. Soc. Perkin Trans. 2: 799–805.
[53] Lampe M, Stavrou M, Bücker HM, Gross J, Bardow A. 2014: Simultaneous optimization of working fluid and process for organic rankine cycles using PC-SAFT. Ind. Eng. Chem. Res. 53: 8821–8830.
[54] Lampe M, Stavrou M, Schilling J, Sauer E, Gross J, Bardow A. 2015: Computer-aided molecular design in the continuous-molecular targeting framework using group-contribution PC-SAFT. Comp. Chem. Eng. 81: 278–287.
[55] Lemberg M, Sadowski G, Gerlach M, Kohls E, Stein M, Hamel C, Seidel-Morgenstern A. 2017: Predicting solvent effects on the 1-dodecene hydroformylation reaction equilibrium. AIChE J. 63: 4576–4585.
[56] Linke S, McBride K, Sundmacher K. 2020: Systematic green solvent selection for the hydroformylation of long-chain alkenes. ACS Sust. Chem. Eng. 8: 10795–10811.
[57] Liu Q, Zhang L, Liu L, Du J, Meng Q, Gani R. 2019: Computer-aided reaction solvent design based on transition state theory and COSMO-SAC. Chem. Eng. Sci. 202: 300–317.
[58] Ljung L. 1999: *System Identification: Theory for the User*. Prentice Hall.
[59] Marcoulaki EC, Kokossis AC. 2000: On the development of novel chemicals using a systematic optimisation approach. Part II. Solvent Design. Chem. Eng. Sci. 55: 2547–2561.
[60] McBride K, Gaide T, Vorholt A, Behr A, Sundmacher K. 2016: Thermomorphic solvent selection for homogeneous catalyst recovery based on COSMO-RS. Chem. Eng. Proc. Proc. Intensif. 99: 97–106.
[61] McBride K, Kaiser NM, Sundmacher K. 2017: Integrated reaction–extraction process for the hydroformylation of long-chain alkenes with a homogeneous catalyst. Comp. Chem. Eng. 105: 212–223.

[62] McBride K, Linke S, Xu S, Sundmacher K. 2018: Computer aided design of green thermomorphic solvent systems for homogeneous catalyst recovery. 13th Intern. Symp. Proc. Sys. Eng. 1783–1788.
[63] Meindersma GW, de Haan AB. 2008: Conceptual process design for aromatic/aliphatic separation with ionic liquids. Chem. Eng. Res. Des. 86: 745–752.
[64] Nentwich C, Engell S. 2019: Surrogate modeling of phase equilibrium calculations using adaptive sampling. Comp. Chem. Eng. 126: 204–217.
[65] Papadopoulos AI, Linke P. 2005: A unified framework for integrated process and molecular design. Chem. Eng. Res. Des. 83: 674–678.
[66] Papadopoulos AI, Linke P. 2006: Efficient integration of optimal solvent and process design using molecular clustering. Chem. Eng. Sci. 61: 6316–6336.
[67] Papadopoulos AI, Linke P. 2009: Integrated solvent and process selection for separation and reactive separation systems. Chem. Eng. Proc. Proc. Intensif. 48: 1047–1060.
[68] Papadopoulos AI, Seferlis P, Linke P. 2017: A framework for the integration of solvent and process design with controllability assessment. Chem. Eng. Sci. 159: 154–176.
[69] Papadopoulos AI, Tsivintzelis I, Linke P, Seferlis P. 2018: Computer-aided molecular design: fundamentals, methods, and applications. In: *Reference Module in Chemistry, Molecular Sciences and Chemical Engineering*. Elsevier.
[70] Pereira FE, Keskes E, Galindo A, Jackson G, Adjiman CS. 2011: Integrated solvent and process design using a SAFT-VR thermodynamic description: High-pressure separation of carbon dioxide and methane. Comp. Chem. Eng. 35: 474–491.
[71] Pistikopoulos EN, Stefanis SK. 1998: Optimal solvent design for environmental impact minimization. Comp. Chem. Eng. 22: 717–733.
[72] Rätze KHG, Jokiel M, Kaiser NM, Sundmacher K. 2019: Cyclic operation of a semi-batch reactor for the hydroformylation of long-chain olefins and integration in a continuous production process. Chem. Eng. J. 377: 120453.
[73] Recker S, Kerimoglu N, Harwardt A, Tkacheva O, Marquardt W. 2013: On the integration of model identification and process optimization. Comp. Aided Chem. Eng. 32: 1021–1026.
[74] Sahinidis NV, Tawarmalani M, Yu M. 2003: Design of alternative refrigerants via global optimization. AIChE J. 49: 1761–1775.
[75] Saltelli A, Ratto M, Andres T, Campolong F, Cariboni J, Gatelli D, Tarantola S. 2008: *Global Sensitivity Analysis*. The Primer. John Wiley & Sons.
[76] Scheffczyk J, Redepenning C, Jens CM, Winter B, Leonhard K, Marquardt W, Bardow A. 2016: Massive, automated solvent screening for minimum energy demand in hybrid extraction–distillation using COSMO-RS. Chem. Eng. Res. Des. 115: 433–442.
[77] Scheffczyk J, Schäfer P, Fleitmann L, Thien J, Redepenning C, Leonhard K, Marquardt W, Bardow A. 2018: COSMO-CAMPD: A framework for integrated design of molecules and processes based on COSMO-RS. Mol. Systems Des. Eng. 3: 645–657.
[78] Schilling J, Tillmanns D, Lampe M, Hopp M, Gross J, Bardow A. 2017: From molecules to dollars: Integrating molecular design into thermo-economic process design using consistent thermodynamic modeling. Mol. Sys. Des. Eng. 2: 301–320.
[79] Schilling J, Horend C, Bardow A. 2020: Integrating superstructure-based design of molecules, processes, and flowsheets. AIChE J. 66: e16903.
[80] Schilling J, Entrup M, Hopp M, Gross J, Bardow A. 2021: Towards optimal mixtures of working fluids: integrated design of processes and mixtures for organic rankine cycles. Renew. Sust. Energy Rev. 135: 110179.
[81] Schuur B. 2015: Selection and design of ionic liquids as solvents in extractive distillation and extraction processes. Chem. Papers. 69: 16.

[82] Siougkrou E, Galindo A, Adjiman CS. 2014: On the optimal design of gas-expanded liquids based on process performance. Chem. Eng. Sci. 115: 19–30.
[83] Sobol I. 2001: Global sensitivity indices for nonlinear mathematical models and their Monte Carlo estimates. In: *Mathematics and Computers in Simulation*. p. 271–280.
[84] Struebing H, Ganase Z, Karamertzanis PG, Siougkrou E, Haycock P, Piccione PM, Armstrong A, Galindo A, Adjiman CS. 2013: Computer-aided molecular design of solvents for accelerated reaction kinetics. Nature Chem. 5: 952–957.
[85] Sundmacher K, Freund H. 2010: Chemical process design: Moving matter elements along optimal travel routes in the thermodynamic state space. PSE Asia 2010: The 5th Intern. Symp. on Design, Operation and Control of Chem. Proc.
[86] Ten JY, Hassim MH, Chemmangattuvalappil NG. 2020: Integration of safety and health aspects in a simultaneous process and molecular design framework. Chem. Eng. Res. Des. 153: 849–864.
[87] US EPA. 2017: Estitmation Programs Interface Suite for Microsoft Windows.
[88] Van Derlinden E, Mertens L, Van Impe JF. 2013: The impact of experiment design on the parameter estimation of cardinal parameter models in predictive microbiology. Food Control. 29: 300–308.
[89] Wang J, Lakerveld R. 2018: Integrated solvent and process design for continuous crystallization and solvent recycling using PC-SAFT. AIChE J. 64: 1205–1216.
[90] Wang J, Zhu L, Lakerveld R. 2020: A hybrid framework for simultaneous process and solvent optimization of continuous anti-solvent crystallization with distillation for solvent recycling. Processes. 8: 63.
[91] White MT, Oyewunmi OA, Haslam AJ, Markides CN. 2017: Industrial waste-heat recovery through integrated computer-aided working-fluid and ORC system optimisation using SAFT- γ Mie. Energy Conv. Manag. 150: 851–869.
[92] Wu C, Bai S, Ansorge-Schumacher MB, Wang D. 2011: Nanoparticle cages for enzyme catalysis in organic media. Adv. Mat. 23: 5694–5699.
[93] Zhang L, Pang J, Zhuang Y, Liu L, Du J, Yuan Z. 2020: Integrated solvent-process design methodology based on COSMO-SAC and quantum mechanics for TMQ (2,2,4-trimethyl-1,2-H-dihydroquinoline) production. Chem. Eng. Sci. 226: 115894.
[94] Zhou T, Lyu Z, Qi Z, Sundmacher K. 2015b: Robust design of optimal solvents for chemical reactions – A combined experimental and computational strategy. Chem. Eng. Sci. 137: 613–625.
[95] Zhou T, McBride K, Zhang X, Qi Z, Sundmacher K. 2015a: Integrated solvent and process design exemplified for a Diels-Alder reaction. AIChE J. 61: 147–158.
[96] Zhou T, Wang J, McBride K, Sundmacher K. 2016: Optimal design of solvents for extractive reaction processes. AIChE J. 62: 3238–3249.
[97] Zhou T, Zhou Y, Sundmacher K. 2017: A hybrid stochastic–deterministic optimization approach for integrated solvent and process design. Chem. Eng. Sci. 159: 207–216.
[98] Zhou T, Song Z, Zhang X, Gani R, Sundmacher K. 2019: Optimal solvent design for extractive distillation processes: A multiobjective optimization-based hierarchical framework. Ind. Eng. Chem. Res. 58: 5777–5786.
[99] Zhou T, McBride K, Linke S, Song Z, Sundmacher K. 2020: Computer-aided solvent selection and design for efficient chemical processes. Curr. Opi. Chem. Eng. 27: 35–44.